

This item was submitted to Loughborough's Institutional Repository (<https://dspace.lboro.ac.uk/>) by the author and is made available under the following Creative Commons Licence conditions.



For the full text of this licence, please go to:
<http://creativecommons.org/licenses/by-nc-nd/2.5/>

1 **Preferential dust sources: a geomorphological classification designed**
2 **for use in global dust-cycle models.**

3

4 Joanna E. Bullard¹, Sandy P. Harrison^{2,3}, Matthew C. Baddock⁴, Nick Drake⁵,
5 Thomas E. Gill⁶, Grant McTainsh⁷, Youbin Sun⁸

6 1: Department of Geography, Loughborough University, Leicestershire, LE11 3TU
7 UK. Email: j.e.bullard@lboro.ac.uk

8 2: School of Geographical Sciences, University of Bristol, Bristol, UK

9 3: School of Biological Sciences, Macquarie University, North Ryde, NSW 2109,
10 Australia.

11
12 4: Department of Environmental Sciences, University of Virginia, Charlottesville, USA

13 5: Department of Geography, King's College London, UK

14 6: Department of Geological Sciences, University of Texas at El Paso, Texas, USA

15 7: Griffith School of Environment, Griffith University, Brisbane, Australia

16 8: Institute of Earth Environment, Chinese Academy of Sciences, Xi'an, China

17

18

19

20

21 **Abstract**

22 We present a simple theoretical land-surface classification that can be used to
23 determine the location and temporal behaviour of preferential sources of terrestrial
24 dust emissions. The classification also provides information about the likely nature of
25 the sediments, their erodibility and the likelihood that they will generate emissions
26 under given conditions. The scheme is based on the dual notions of geomorphic type
27 and connectivity between geomorphic units. We demonstrate that the scheme can be
28 used to map potential modern-day dust sources in the Chihuahuan Desert, the Lake
29 Eyre Basin and the Taklamakan. Through comparison with observed dust emissions,
30 we show that the scheme provides a reasonable prediction of areas of emission in
31 the Chihuahuan Desert and in the Lake Eyre Basin. The classification is also applied
32 to point source data from the western Sahara to enable comparison of the relative
33 importance of different land surfaces for dust emissions. We indicate how the
34 scheme could be used to provide an improved characterization of preferential dust
35 sources in global dust-cycle models.

36

37 **1 Introduction**

38 Mineral aerosol plays an important role in the land-atmosphere-ocean system. Wind
39 erosion causes removal of fine particles (usually <100 µm in diameter) from the land
40 surface, affecting soil moisture holding capacity and nutrient content [e.g. *McTainsh*
41 *and Strong*, 2007; *Li et al.*, 2007]. Whilst suspended in the atmosphere, mineral
42 aerosol has a range of direct and indirect effects on regional and global climate
43 [*Forster et al.*, 2007], including changing radiative forcing [e.g. *Haywood and*
44 *Boucher*, 2000; *Yoshioka et al.*, 2007], cloud properties [*Rosenfeld et al.*, 2001] and
45 the chemistry of precipitation [*Dentener et al.*, 1996], suppressing tropical cyclone
46 formation [*Sun et al.*, 2007] and possibly increasing hurricane intensity [*Foltz and*
47 *McPhadden*, 2008]. Dust deposited over land can affect soil development, soil fertility
48 and geomorphic processes [e.g. *McFadden et al.*, 1987; *Muhs et al.*, 2007]. Dust may
49 regulate phytoplankton activity in the oceans [*de Baar et al.*, 2005; *Wolff et al.*, 2006]
50 and has been (inconclusively) linked to disease and bleaching in corals [*Shinn et al.*,
51 2000]. Dust emissions even from small, localised sources can have an important
52 impact on health [*Griffin and Kellogg*, 2004] and through creating hazardous
53 conditions for traffic [*Ashley and Black*, 2008]. The impact of dust in the Earth's
54 system depends partly on the location, magnitude, frequency and intensity of dust
55 emissions and partly on the size, shape and mineralogy of the emitted dust particles
56 [*Jickells et al.*, 2005; *Durant et al.*, 2009]. Although dust concentration and particle
57 characteristics change during transport [*Desboeufs*, 2005; *Schütz et al.*, 1981], they
58 are initially determined by the terrestrial sources from which the particles are
59 entrained.

60 Models developed to investigate the impacts of climate changes on atmospheric dust
61 loading explicitly simulate dust emission, atmospheric transport, and removal by wet
62 and dry deposition. The largest difference between these models lies in the treatment
63 of emissions: some models parameterize emissions solely as a function of wind
64 speed and surface roughness [e.g. *Tegen and Fung*, 1994; *Ginoux et al.*, 2001],
65 while other schemes explicitly include sandblasting as a mode of dislodging particles
66 [e.g. *Shao et al.*, 1993; *Alfaro and Gomes*, 2001; *Zakey et al.*, 2006]. Many models
67 now include the control of seasonally-varying vegetation cover on dust emission,
68 either by prescribing vegetation cover [e.g. *Mahowald et al.*, 1999; *Zender et al.*,
69 2003; *Mahowald et al.*, 2006] or through explicitly simulating vegetation dynamics
70 and phenology [e.g. *Werner et al.*, 2003].

71 Field and satellite observations have shown that dust sources are highly localized

72 spatially [*Middleton et al.*, 1986; *Ginoux et al.*, 2001; *Prospero et al.*, 2002; *Mahowald*
73 *et al.*, 2003; *Washington et al.*, 2003]. Models of the dust cycle that define source-
74 area erodibility, using observations of surface reflectance [*Grini et al.*, 2005] or
75 surface roughness [*Koven and Fung*, 2008], implicitly include these preferential
76 sources. Prescription of land-surface properties is of limited applicability, however,
77 when the aim is to model emissions under radically different climate conditions such
78 as those which pertained in the geologic past or which could arise with global
79 warming in the future. An alternative modeling approach has been to define the
80 spatial distribution of preferential dust sources such as topographic depressions
81 [*Ginoux et al.*, 2001] and dry lake basins [*Tegen et al.*, 2002] explicitly. Soil properties
82 or dust fluxes are then changed to ensure increased emissions from these areas.
83 The inclusion of preferential sources produces a more realistic simulation of
84 emissions, both under modern and past climate states, although model output is
85 significantly affected by the way in which land-surface characteristics are
86 incorporated [*Uno et al.*, 2006, *Yin et al.*, 2007]. However, current modeling
87 approaches still do not capture the small-scale spatial and temporal variability in
88 emissions apparent from observations. Furthermore, the identification of significant
89 emissions from surfaces not previously considered important, such as alluvial fans in
90 the Sahara [*Schepanski et al.*, 2007], suggests that current modeling approaches
91 may neglect some preferential sources. A more comprehensive treatment of the
92 geomorphic controls on emission is therefore required to improve the performance of
93 dust-cycle models.

94 It would be possible to adopt a purely empirical approach to identifying potential
95 sources and characterizing the spatial and temporal heterogeneity in emissions using
96 remotely sensed data. Such an approach has been adopted in several papers
97 [*Schepanski et al.*, 2007; *Bullard et al.*, 2008] but it has a number of limitations.
98 Firstly, although the length of the record is increasing and the quality of data
99 improving, remote-sensing products are only available for a limited number of years.
100 Some dust sources are active very sporadically [e.g. *Bessagnet et al.*, 2008; *Sharma*
101 *et al.*, 2009] and may not have been active during the period covered by the remote
102 sensing record. Secondly, the relative importance of different sources as
103 reconstructed from remotely-observed emissions is determined by prevailing
104 meteorological conditions during the observation period – again, this may not
105 represent the full range of environmental conditions experienced in any region. Thus,
106 an empirical classification will not be a reliable guide to emissions under changed
107 conditions such as those experienced in the geologic past or expected in the 21st

108 century. Thirdly, it is difficult to extend an empirical classification beyond the area for
109 which it was developed, making it less suitable for incorporation in a global modeling
110 framework and particularly a framework designed to be applied with climate-change
111 scenarios. We have therefore chosen an alternative approach of developing a
112 theoretical classification of different types of geomorphological surface with respect
113 to their potential as dust sources, drawing on knowledge accumulated through
114 extensive field mapping of land surface characteristics and information on how these
115 surfaces react under different meteorological and environmental conditions gathered
116 during many years of research.

117 Studies characterizing the geomorphology and surface properties of dryland regions,
118 and relating these to the occurrence and frequency of dust emissions [e.g. *Reheis*
119 *and Kihl*, 1995; *Bullard et al.*, 2008; *Wang et al.*, 2006; *Wang et al.*, 2008b] have
120 provided a reasonably good understanding of the geomorphic controls on dust
121 sources and how these will affect both the spatial extent and the temporal behavior of
122 sources. In this paper, we present a synthesis of current knowledge about the
123 geomorphic controls on dust sources, and develop a conceptual model of how
124 different geomorphic sources will affect the temporal variability in dust emissions. We
125 demonstrate that the resulting classification scheme can be used to map potential
126 modern-day dust sources in three regions: the Chihuahuan Desert, the Lake Eyre
127 Basin and the Taklamakan. We test how well the conceptual model predicts emission
128 sources in the Chihuahuan Desert and in the Lake Eyre Basin through comparison
129 with observed dust emissions. We also present a preliminary assessment of its
130 application to the western Sahara, by using point source data to enable comparison
131 of the relative importance of different land surfaces for dust emissions. Finally, we
132 suggest ways in which a classification scheme based on our conceptual model could
133 be used to derive an improved characterization of preferential sources for dust-cycle
134 modeling and conclude with suggestions about how this scheme could be
135 implemented in a modeling framework. The focus of this paper is the relationship
136 between surface geomorphology and sedimentology and dust emissions – we have
137 explicitly not tried to link this to other variables controlling emissions, such as wind
138 velocity, vegetation cover or human land use, because these variables are already
139 treated in global dust models.

140

141 **2. Conceptual Model of the Geomorphic Controls on Dust Sources**

142 **2.1. Geomorphic Characteristics and Dust Emissions**

143 Although any terrestrial surface with a supply of suitable-sized sediment and
144 appropriate wind regime can be a dust source, most dust emissions are from arid
145 (<250 mm yr⁻¹ rainfall) inland drainage basins [*Middleton et al.*, 1986; *Prospero et al.*,
146 2002; *Washington et al.*, 2003]. Dryland inland basins are extensive and their surface
147 characteristics and geomorphic dynamics encompass many different sedimentary
148 environments including stone pavement (also known as gobi, reg or gibber),
149 unconsolidated aeolian deposits, endorheic depressions, fluvial, alluvial and
150 groundwater-dominated systems, and consolidated or sealed surfaces such as
151 evaporite crusts, duricrusts or bedrock. With the probable exception of consolidated
152 surfaces [*Gillette*, 1999; *Callot et al.*, 2000], all of these units have the potential to
153 emit dust. However, they vary both in their relative importance as emission sources,
154 and in the spatial and temporal patterns of emissions because the geomorphological
155 characteristics of the units affect the amount of sediment available for wind erosion.

156 Studies in different regions have shown that the relationship between geomorphology
157 and dust sources is not simply a function of gross geomorphic type. *Wang et al.*
158 [2006] showed that most dust storms in northern China originate in gobi (stony
159 deserts), whilst *Sweeney et al.* [2006] found stone pavements in the Mojave Desert
160 had the lowest dust emissions. Similarly, *Prospero et al.* [2002] found that dunefields
161 were not major dust sources, but dust emissions have been reported following the
162 reactivation of semi-stabilized dunes [*Sweeney et al.*, 2006; *Bullard et al.*, 2008;
163 *McGowan and Clark*, 2008] and from dunefields where river systems inundate
164 interdunal areas with fresh sediment that is subsequently desiccated and deflated
165 [*Bullard et al.*, 2008; *Wang et al.*, 2006]. Iron oxide and other fine weathering
166 coatings on dune sands are also potential dust sources [e.g. *Bullard and White*,
167 2005; *Bullard et al.*, 2007; *Crouvi et al.*, 2008]. *Reheis and Kihl* [1995] found that in
168 the Mojave Desert and southern Great Basin of the southwestern USA, playa and
169 alluvial sources produce almost the same amount of dust per unit area, but the
170 greater surface area of the latter means the total volume of dust emitted from alluvial
171 deposits is much higher. *Reheis* [2006] also found that alluvial sources in this region
172 are the primary dust sources during drought, whilst playas are the primary dust
173 producers during wetter periods.

174 The vegetation-free expanse of flat, fine-sediment dominated ephemeral lakes can
175 be an important source of dust in terms of both intensity (emissions per unit area)
176 and magnitude [e.g. *Reheis*, 1997, 2006; *Mahowald et al.*, 2003; *Prospero et al.*,
177 2002; *Washington et al.*, 2003; *Bullard et al.*, 2008]. Several studies have
178 demonstrated the importance of sand-sized sediment in releasing dust to the

179 atmosphere from consolidated or compacted clays or silts [*Cahill et al.*, 1996; *Gillette*
180 *and Chen*, 2001; *Shao et al.*, 1993; *Grini and Zender*, 2004]. These coarse saltators
181 can trigger the release of fine dust particles from the bed and, through the process of
182 aeolian abrasion, generate additional fine particles [*Gomes et al.*, 1990]. On
183 ephemeral lake beds, coarse saltators may be provided by adjacent sand dunes
184 [*Stout*, 2003], or deposition of fine sands following flooding [*McTainsh et al.*, 1999].
185 This emphasizes the importance of understanding not only the sedimentary
186 environment of a particular landform, but also the degree of connectivity with
187 adjacent landforms. Connectivity also influences sediment supply and can result in
188 differences in emissions from similar geomorphic features from different regions
189 [*Bullard and McTainsh*, 2003].

190

191 **2.2 Controls of Temporal Variation in Dust Sources**

192 The importance of different geomorphic units as dust sources varies in space and
193 time depending on soil moisture, vegetation cover, the presence of biological crusts,
194 mechanical disturbance (e.g. by animals or human activities) and wind strength. With
195 the exception of mechanical disturbance and crusts, these controls are already
196 incorporated in global models and so are not explicitly considered in our dust source
197 mapping scheme. However, there are additional controls of dust emission brought
198 about through the interaction of climate and landscape on sediment availability.
199 These interactions can be described in terms of the aeolian sediment-system
200 response framework developed by *Kocurek* [1998; see also *Kocurek and Havholm*,
201 1993]. In this conceptual model, sediment production peaks during humid conditions
202 when weathering, and fluvial transport and sorting, are enhanced but aeolian
203 sediment availability and transport capacity are low due to the presence of
204 vegetation. As conditions become more arid, sediment production declines and
205 sediment availability to the wind plus transport capacity increase (Figure 1). Applying
206 this conceptual framework to dust emissions, a system can be in one of three states:
207 supply-limited, where emissions are limited by lack of suitable sediment; availability-
208 limited, where there is sediment in the system but it is not readily entrainable either
209 due to vegetation cover or soil moisture levels; or transport-capacity limited, where
210 sediments are available but wind energy is too low to entrain particles. Some
211 attempts have been made to classify regional dust sources using similar principles.
212 *Zender and Kwon* [2005] identified relationships among precipitation, dust loading
213 and vegetation cover for dust source areas that highlighted regions where dust

214 emissions were supply limited. *Mahowald et al.* [2007] also found regions where
215 higher water availability was associated with higher dust emissions and suggested
216 that this reflected increased sediment delivery to emission zones. The division
217 between supply-limited, availability-limited and transport-capacity limited is not
218 perfect because the states are not mutually exclusive (for example there is a strong
219 relationship between vegetation cover and the threshold wind strength required to
220 entrain particles), however it does provide a useful way to account for some aspects
221 of temporal variability in dust emissions.

222

223 <Figure 1>

224

225 **2.3 Sediment Texture**

226 Attribution of appropriate sediment texture information is important for characterizing
227 potential dust sources. In most dust-cycle models, the characteristics of the surface
228 material are specified from global soils data sets such as the various versions of the
229 FAO soil data set [*Zobler*, 1986; *IUSS Working Group WRB*, 2007] at the spatial
230 scale of the model (generally 0.5°x 0.5° to 1°x 1°). The textural information used to
231 classify soils does not fit particularly well with the particle sizes that are susceptible to
232 wind erosion, or those capable of generating such particle sizes through
233 sandblasting. Wind is highly size selective and tends to only carry particles <2000 µm
234 diameter by saltation or suspension: this incorporates sediments that are described
235 as sand (63-2000 µm, or 50-2000 µm), silt (4-63 µm, or 2-50 µm), and clay (<4 or <2
236 µm) in traditional grain-size classifications (size boundaries according to *Wentworth*,
237 [1922] and *Urquhart*, [1959] respectively). Furthermore, the soil texture data refers to
238 particle sizes determined using dispersed or disaggregated sediments which may not
239 reflect particle sizes in the field [e.g. *Chatenet et al.*, 1996]. Fine particles may be
240 present, for example, as sand-sized aggregates that can be broken down into
241 component dust-sized grains during transport or sandblasting, or as clay or metal
242 oxide deposits on the surfaces of sand grains, which can be removed by abrasion to
243 form dust. The importance of sandblasting for dust production is expressed in the
244 observed relationship between vertical dust flux F , and horizontal mass flux
245 (saltation), q [*Shao et al.*, 1993; *Gillette et al.*, 1997; *Okin*, 2005]. The effectiveness of
246 abrasion in generating dust for a given surface is represented by the ratio of dust
247 emission to horizontal sediment flux ($k = F/q$). The k factor varies between different

248 surfaces, being controlled by local sediment properties such as texture, crusting and
249 moisture. Finally, although the sorting of material may be important in determining
250 susceptibility to wind erosion, information on sorting is rarely given in soil datasets.

251 Grain size, the presence of aggregates, and sorting are highly variable, both within
252 sedimentary environments and between different sedimentary environments.
253 Nevertheless, there are some basic relationships between these properties and the
254 more important geomorphic types in dust source regions. We have therefore
255 developed a simple description of broadly defined sediment classes (Table 1) that
256 can be directly related to specific geomorphic types in terms of their susceptibility to
257 wind erosion and their potential for dust generation. In general, erodibility is reduced
258 by the admixture of coarse gravel-sized particles but in some situations coarser
259 (sand-sized) particles are required to promote deflation of cohesive fine-grained
260 material.

261

262 <Table 1>

263

264 **3. Development of a Global Scheme**

265 **3.1 Basic Criteria**

266 There is no global database of land surface characteristics including soil type,
267 texture, organic content, particle size and sorting, sediment budget, sedimentary
268 environment and geomorphology. Reasonably high quality data on some or all of
269 these variables are available for some regions. However, each regional study tends
270 to use different methods of data collection and compilation, different classification
271 schemes and different mapping resolutions. These differences can be further
272 compounded if the area of interest extends across national boundaries [e.g. *Baddock*
273 *et al.*, 2011]. This poses problems in reconciling the different datasets into a single,
274 global dataset that would be suitable for dust-cycle modeling.

275 We initially considered the types of geomorphic features that are characteristic of arid
276 and semi-arid regions, differentiating them in terms of mode of formation and likely
277 sedimentological characteristics. This type of geomorphic classification and mapping
278 has been conducted by others; early studies include those by *Raisz* [1952] and
279 *Clements et al.* [1957], more recent work has been carried out by *Callot* [2000] and

280 *Ballantine et al.* [2005]. Our geomorphological types cover the same range of
281 landscape features as these studies.

282

283 Our focus in developing a new scheme for dust source mapping has been to ensure
284 that the data required to apply it are easily available, globally-consistent and
285 verifiable. Thus, we sought to create a scheme using a limited number of easily
286 recognizable geomorphological units, the location and extent of which could be
287 defined using e.g. satellite remote sensing, aerial photography, topographic, soil and
288 geological maps and field data. The use of remote-sensed data or field mapping
289 means that the scheme is based on surface characteristics rather than the nature of
290 the underlying sediments. In some situations, the underlying sediments could have
291 been important for dust production in the past or provide a future source of dust, but
292 including this stratigraphic information is beyond the scope of a globally-applicable
293 scheme. Although the boundaries between the different geomorphologies are clearly
294 delimited in some cases (e.g. perennial lakes) in other cases there is a gradual
295 transition between different types (e.g. sandy aeolian deposits may grade into sand
296 sheets or loess over distances ranging from a few to hundreds of kilometers: *Crouvi*
297 *et al.*, [2008]). This introduces a certain amount of subjectivity into the mapping that
298 is unavoidable. In developing the scheme, we have borne in mind that its primary
299 purpose is to provide a basis for global mapping of dust source types which could
300 then be used to prescribe dust source types in global dust-cycle models. This has led
301 to a simplification of the micro-scale complexity which characterizes specific arid and
302 semi-arid regions, but a more complex classification scheme would be difficult to
303 operationalize either in a mapping or a modeling context.

304

305 **3.2 Geomorphic Types**

306 We identified seven geomorphic types that are commonly found in arid and semi-arid
307 regions, which differ in terms of surface characteristics influencing their susceptibility
308 to aeolian erosion, and which matched our criterion for being readily identifiable using
309 remotely-sensed information. The seven basic types are lakes [1], high relief alluvial
310 deposits [2], low relief alluvial deposits [3], stony surfaces [4], sand deposits [5], loess
311 [6] and low emission surfaces [7]. These were further sub-divided (Table 2) to reflect
312 perceived differences within each basic type in the spatial and/or temporal variability
313 of emissions. The resultant classification relies primarily on our collective field
314 experience, including explicit field studies of the relationships between geomorphic
315 setting and dust emission, as well as our evaluation of the literature on dust

316 emissions from key regions. In the sections below, we examine each of the
317 geomorphic types (and sub-types) in turn in order to explain the reasoning behind
318 their differentiation in terms of their importance and behaviour as potential dust
319 sources. Our subsequent analyses of the application of this classification in different
320 regions (see Results) can be seen as a test of our initial, somewhat theoretically-
321 based, classification.

322

323 <Table 2>

324

325 **3.2.1 Lakes [1a-d]**

326 Perennial (wet) lakes [1a] may contain sediments suitable for wind erosion but the
327 presence of water means that the system is availability limited. Perennial lakes can
328 be an efficient trap of fine sediments and hold a detailed record of past periods of
329 dust activity [e.g. *Muhs et al.*, 2003]; they are also potential future dust sources if fully
330 or partially desiccated [*Gill*, 1996]. Delimitation of perennial lakes using remote
331 sensing is usually reliable because water has significantly different spectral
332 properties from vegetation or exposed lacustrine sediments [*Drake and Bryant*,
333 1994].

334 Ephemeral lakes [1b] are one of the most important dust sources globally [*Prospero*
335 *et al.*, 2002; *Washington et al.*, 2003]. In general, these lakes have been perennial at
336 some stage in the past, and thus contain considerable quantities of fine-grained
337 material of fluvial, groundwater-derived and/or biogenic origin. Some of these
338 materials are particularly productive: diatomites, for example, are very erodible as
339 their silicate skeletons are readily abraded to dust size particles by sandblasting
340 [*Warren et al.*, 2007]. The diatomite deposits of the Bodélé Depression in Chad are
341 the world's biggest dust source in terms of fluxes [*Washington et al.*, 2006].

342 The importance of lakes without a plentiful store of fine-grained sediment as dust
343 sources depends on the delivery of new sediment through ephemeral flooding or
344 fluvial activity. Flow deceleration when rivers enter a lake causes rapid deposition of
345 coarse sediment near the lake margin and concentrates fines increasing towards the
346 centre of the basin. Coarser material settles out of the water column more rapidly
347 than finer material depositing a fining upwards sequence. Following desiccation,
348 these fine sediments will deflate and may expose coarser material that promotes
349 sandblasting [*Cahill et al.*, 1996]. Ultimately, deflation may strip away the fines and

350 lead to the development of a coarse lag deposit, causing the system to switch to
351 being availability-limited.

352 When groundwater levels are close to the surface of the lake bed (or deflation lowers
353 the surface of the lake bed to the groundwater table) increased cohesion may reduce
354 sediment availability. Salts precipitated from near-surface groundwater have different
355 effects on dust production depending on their chemistry: sulfate and carbonate
356 evaporites can create 'soft puffy' surfaces or loose fine salt deposits that are prone to
357 erosion [Cahill *et al.*, 1996; Katra and Lancaster, 2008; Reynolds *et al.*, 2007; Rojo *et*
358 *al.*, 2008], while sodium chloride-rich evaporites tend to form hard, cemented layers
359 reducing sediment erodibility [Handford, 2006].

360 Sediments exposed on permanently dry lake beds may be consolidated by salts
361 cementing the particles together [1c] or unconsolidated [1d]. Assuming no change in
362 other environmental factors (such as particle sorting, groundwater level or surface
363 moisture availability), deflation of unconsolidated sediments of appropriate size (or
364 aggregate size) is effectively limited only by transport capacity until all sediments are
365 deflated and the system becomes supply-limited. Consolidated dry lake sediments
366 are availability-limited.

367

368 **3.2.2 High Relief Alluvial Deposits [2a-d]**

369 Alluvial deposits are sub-divided according to relief, armouring and incision. Relief (or
370 gradient) determines the energy available in the fluvial system; it also affects the
371 sediment type such that high relief systems generally comprise coarser material than
372 low relief systems. Although there is no universal threshold in terms of gradient
373 dividing low and high relief systems, typically alluvial systems with a gradient of less
374 than 2-3° are classified as low relief whereas those with steeper gradients are high
375 relief. In practice these values are always used in conjunction with interpreting the
376 geomorphic signature - alluvial plains are easily recognizable and are classified as
377 low relief alluvial deposits while high relief surfaces such as fans, piedmont slopes
378 and bajada also have a distinct geomorphologically-recognizable signature.
379 Armouring of the surface of an alluvial deposit by coarse particles reduces potential
380 dust emissions. Channel incision affects the floodplain extent and frequency of
381 inundation, which is the main mechanism by which sediments are transferred from
382 the fluvial to the aeolian system [Bullard and McTainsh, 2003]. The numerous ways

383 in which these three variables combine mean that alluvial deposits contain a wide
384 range of sediment textures.

385

386 Armoured alluvial deposits associated with high relief [2a and 2b] are typically
387 availability-limited due to poor sorting, a relatively low silt content and the presence of
388 armoured surfaces which increases surface roughness and lowers wind erosion
389 potential. In contrast, unarmoured, high relief, alluvial deposits [2c and 2d] are more
390 likely to be dust sources but may be supply-limited. In this case, significant dust
391 emissions only occur after periodic rains bring fresh sediment into the system
392 (although over long periods weathering may also supply some fine sediments; *Viles*
393 *and Goudie*, [2007]). When sediment textures are very mixed, alluvial fans can be
394 dust sources if there is active reworking to maintain a supply of fine material at the
395 surface or to prevent the surface from becoming armoured [*Derbyshire et al.*, 1998,
396 *Wang et al.*, 2006, 2008b, *Reheis*, 2006]. Topographic enhancement of winds can
397 also play an important role in dust entrainment, as in the foothills of the Air Mountains
398 in the Sahara [*Karam et al.*, 2009; *Schepanski et al.*, 2007].

399

400 **3.2.3 Low Relief Alluvial Deposits [3a-d]**

401 Alluvial deposits associated with low relief may still contain gravels that can cause
402 armouring. Armoured surfaces are present on palaeodeltas associated with the
403 Jilantai dry lake, for example [*Yang et al.*, 2008]. Low relief alluvial deposits may also
404 be incised, limiting any replenishment of fines by floodwaters [3a and 3b]. The low
405 relief category also includes braided fluvial systems and outwash plains in paraglacial
406 and periglacial landscapes. These regions can be significant dust sources [*McKenna*
407 *Neuman and Gilbert*, 1986; *Muhs et al.*, 2003; *Nickling*, 1978] with the timing of dust
408 emissions linked to meltwater flooding and seasonal or local availability of suspended
409 sediment [Bullard and Austin, 2011] or, over longer time periods, to the formation or
410 drainage of proglacial lakes [*Sugden et al.*, 2009].

411 Unarmoured, low gradient alluvial surfaces [3d] are either transport-capacity limited
412 or, if they are vegetated, availability-limited. In the Okavango Delta, for example,
413 peak periods of dust deflation occur during drought years when vegetation cover is
414 reduced [*Krah et al.*, 2004]. Similarly, in the extensive unarmoured floodplains in
415 Australia's Channel Country fine sediment supply is related to occasional high

416 magnitude flood events; dust emissions here are strongly controlled by both
417 sediment supply and availability through vegetation [McTainsh and Strong, 2007].

418

419 **3.2.4 Stony Surfaces [4]**

420 Although colluvial deposits [7] and alluvial deposits [2, 3] may have stony surfaces,
421 stony surfaces *sensu stricto* are low angle, stone-mantled surfaces formed by a
422 range of different processes [McFadden *et al.*, 1987; Adelsberger and Smith, 2009].
423 They are a store of relatively fine sediment overlain by a thin surface mantle of
424 gravels (>2000 µm diameter) [Springer, 1958; Cooke, 1970; Peterson, 1980]. The
425 underlying material is typically dominated by silt but sand-sized material does occur
426 in some locations [e.g. Marticorena *et al.*, 1997; Pelletier *et al.*, 2007]. The coarse
427 surface layer limits aeolian erosion of the underlying finer fraction such that these are
428 availability-limited sedimentary environments. These units can emit dust, however, if
429 the surface is significantly disturbed or under strong winds [e.g. Belnap and Warren,
430 2002].

431

432 **3.2.5 Sand Deposits [5a-b]**

433 Sand deposits are sub-divided into sand sheets and aeolian sand dunes. Sand
434 sheets [5a] are areas of low relief sandy deposits. The size and sorting of the
435 sediments makes them susceptible to wind erosion but, in many cases, aeolian
436 entrainment is limited by vegetation, coarse sands or the level of the water table.

437 In contrast to sand sheets, aeolian sand dunes [5b] are a wind-worked deposit with
438 distinct relief. The contribution of sand dunes to dust emissions depends on type,
439 activity level, and palaeoenvironmental history. Active, young or small sand dunes
440 with a relatively rapid turnover of sand are unlikely to be major or persistent dust
441 source because they contain little fine material. Large, more stable or older dunes
442 may accumulate fines within the dune structure due to weathering or, in semi-arid
443 regions, through in-wash of finer particles by precipitation. Dunes in hyper-arid
444 regions are less likely to contain fine material than those in semi-arid and temperate
445 zones; large areas of the latter have partial vegetation cover which, although it will
446 trap fine wind-blown sediments, also reduces sediment availability unless it is
447 disturbed. Dune activity and palaeohistory are not easy to detect from remote
448 sensing, consequently here all dunes are classified in a single category [5b].

449

450 **3.2.6 Loess [6]**

451 Loess is a depositional landform of silt and clay-sized dust particles. There is often a
452 marked gradient in sediment size with coarser sediments near the dust source and
453 finer sediments further away, and there may be a wide transitional zone from sand to
454 silt and clay-sized material. Loess can become a significant dust source during
455 periods of reduced vegetation or disturbance.

456

457 **3.2.7 Low Emission Surfaces [7]**

458 Bedrock, steep rocky slopes, duricrusts, and permanent snow and ice cover in cold
459 deserts, are surfaces where sediment supply and/or sediment availability are typically
460 low to zero and thus emissions are low.

461

462 **4 Application of Geomorphic Classification to Major Dust Source Regions**

463 The applicability of the geomorphic classification scheme was first tested in two
464 regions (the Chihuahuan Desert and Lake Eyre Basin); we performed more limited
465 tests in a further two regions (the Sahara west of 17°E and Taklamakan Deserts) to
466 demonstrate the scheme's global potential. All four regions have previously been
467 examined in terms of the relationship between dust sources and surface
468 geomorphology [*Wang et al.*, 2006; *Drake et al.*, 2008; *Bullard et al.*, 2008; *Lee, et*
469 *al.*, 2009] – though using very different classification approaches -- and differ in terms
470 of the relative importance of different geomorphological types and the temporal
471 variability of the dust sources (Table 3). Attempting to apply the geomorphic
472 classification scheme outlined in this paper in all four regions is a first step towards
473 establishing the feasibility of a common mapping protocol.

474 The Chihuahuan Desert (CD), North America and Lake Eyre Basin (LEB), Australia
475 were mapped in detail. The mapping scheme was then evaluated by using dust point
476 source data for the CD and LEB and overlying this on the geomorphic maps to
477 determine whether or not the actual distribution of dust sources coincided with
478 theoretically predicted areas of high or medium emissions. The Taklamakan (TAK),
479 China was mapped using the mapping scheme but, as no point source data were
480 available from the region, the map was then evaluated using existing literature. The
481 western Sahara (SAH), North Africa was not mapped in detail because of its large
482 size and resource constraints, but the mapping scheme was applied to an existing
483 data set of dust point source data.

484

485 **4.1 Geomorphic Mapping**

486 The spatial extent and the distribution of the seven geomorphic classes (and their
487 sub-classes) were mapped across the CD, the LEB and the TAK by applying the
488 scheme to an existing digital base map of polygons which had been established for
489 each region. Each polygon was then attributed to a geomorphic class from Table 2.
490 The allocation was based on interpretation of remote sensing imagery. This
491 allocation was cross-checked against secondary sources, including regional maps
492 and literature. This kind of mapping is a standard practice in geomorphology and the
493 results are generally robust between operators; cross-checking against secondary
494 sources provides a further check on this robustness. This procedure resulted in a
495 vector polygon map for each region, suitable for analysis in a geographical
496 information system.

497

498 The Chihuahuan Desert covers 322,450 km² of southwestern North America in
499 Mexico and the USA as delineated climatically by *Schmidt* [1979]. There are no
500 detailed land unit maps that continue across the international border so a base map
501 was compiled using 1:1,000,000 landform/landscape unit maps obtained from the
502 Mexican Sistema de Topoformas dataset [*INEGI*, 2001] and 1:250,000 soils maps
503 produced by the US Department of Agriculture's Natural Resource Conservation
504 Service [*USDA-NRCS*, 2006]. A base map covering the entire Chihuahuan Desert
505 was created by merging the USA and Mexican primary source maps and adjoining
506 common polygons were unified across the international border. The positional
507 accuracy of the polygon boundaries is ≈ 250 m for the Mexican data and varies from
508 250 m to 1 km for the USA data [*USDA-NRCS*, 2011]. The smallest polygon on the
509 base map has an area of 1 km². Each polygon in the base map was then assigned to
510 one of the 17 different geomorphic sub-classes described in Table 2 and adjacent
511 polygons with the same geomorphic characteristics were merged with the result that
512 the smallest polygon increased in size to 2 km². Where available and appropriate,
513 metadata provided with the base maps were used to assist with classification of land
514 surfaces (for example wet lakes [1a]) but assignment of geomorphic characteristics
515 was primarily achieved using the NASA Geocover mosaic created from Landsat
516 ETM+ (at 14.5 m spatial resolution; *Tucker et al.*, 2004), the authors' field knowledge,
517 dedicated ground-truthing sorties and published literature [*Baddock et al.*, 2011].
518 The boundaries of the geomorphic classes were fine-tuned using these data sources

519 which helped to improve the positional accuracy; this was especially important in
520 areas of complicated geomorphology and where sub-types within the scheme (e.g.
521 lake sub-types) were in close proximity to one another.

522

523 The base map of polygons used for the classification of the 1.14 million km² Lake
524 Eyre Basin, defined by the watershed boundary, was the 1:1,000,000 Surface
525 Geology of Australia base map. This dataset is compiled from a number of different
526 sources and the polygon boundaries have a positional accuracy ranging from 200 m
527 to 1 km depending on the quality and date of the original input data [*Raymond and*
528 *Retter, 2010*]. The smallest polygon in the base map has an area of 0.25 km². Each
529 polygon in the LEB map was then assigned to one of the 17 different geomorphic
530 sub-classes and adjacent commonly-classified polygons were merged. Although
531 most of the geomorphologically-assigned polygons increased in size, geomorphology
532 is spatially very variable in some areas of the watershed and the smallest polygon
533 still had an area of 0.25 km². Where available and appropriate, metadata provided
534 with the base maps were used to assist with classification of land surfaces (for
535 example aeolian sand dunes [5b]), however assignment of geomorphic
536 characteristics was primarily achieved using the global NASA Geocover mosaic
537 [*Tucker et al., 2004*], the 1:250,000 digital topographic map series of Australia
538 (positional accuracy ±120 m; Geosciences Australia, 2008), SPOT (Satellite Pour
539 l'Observation de la Terre) data (spatial resolution ≤10 m), the authors' field
540 knowledge and dedicated ground-truthing sorties. The boundaries of the
541 geomorphological type polygons were adjusted where necessary using these higher
542 resolution data sources.

543

544 A 523,545 km² area of the Tarim Basin, encompassing the Taklamakan Desert was
545 mapped using a base map digitised from the geomorphic map by *Tungsheng et al.*
546 [1996]; this was georectified and then the polygon boundaries were checked and,
547 where necessary, modified to include additional detail using other published data
548 [e.g. *Wang et al., 2008a,b*] and SPOT imagery. The positional accuracy of the
549 polygon boundary is estimated to range from 1 km to 20 km, decreasing towards the
550 margins of the mapped area. The geomorphology was mapped at a lower resolution
551 than the other regions, with the smallest polygon being 675 km². Although the original

552 basemap for the Taklamakan was digitised from an existing, and quite detailed,
553 geomorphic map, the allocation of polygons to our scheme was done independently.

554

555 The three maps were produced using ArcGIS (ESRI) and the area of each
556 geomorphic type was calculated. For all maps, where transitions between
557 geomorphic types were identified, the boundary was placed where the dominant type
558 changed. We estimate that the overall error in determining the geomorphic
559 boundaries for CD and LEB is no greater than 1 km.

560

561 **4.2 Dust Source Data**

562 Dust point source data was obtained for the CD, the LEB and SAH (Table 4).
563 Meteorological records from El Paso International Airport, from 1st January 2001 to
564 31st December 2009, were used to identify days in which visibility in the CD was
565 reduced by dust/haze/sand or other aeolian phenomena (excluding smoke, and
566 anthropogenic pollutants). For the LEB all days during the period July 2003 to June
567 2006 were identified when at least one meteorological station within the LEB or within
568 250 km of the watershed recorded a dust-induced visibility reduction to ≤ 1 km
569 [Bullard *et al.*, 2008]. For both regions, we analysed MODIS (Moderate Resolution
570 Imaging Spectroradiometer) images (Terra and/or Aqua) for each different
571 meteorologically-defined dust day and for days where plumes were evident, the
572 upwind source position of the dust plumes was identified through cross-referencing
573 with meteorological data to identify the direction of dust transport. MODIS data has
574 been widely and successfully used to identify dust sources and track dust storms in
575 desert regions [e.g. Gassó and Stein, 2007; McGowan and Clark, 2008; Walker *et*
576 *al.*, 2009].

577 Several techniques have been developed to enhance the dust signal over desert
578 surfaces. A comparison of four of these techniques, and two aerosol products
579 (MODIS Deep Blue and OMI AI; Ozone Monitoring Instrument Absorbing Aerosol
580 Index) concluded that approaches using brightness temperature difference (the
581 difference between the 11 and 12 μm bands; Ackerman, [1997]) were the most
582 consistently reliable for accurate source identification [Baddock *et al.*, 2009].
583 Although this approach makes it easier to identify the sources of dust plumes, it
584 involves a loss of precision because the highest spatial resolution MODIS data to

585 which it can be applied is 1 x 1 km. This loss of precision is not important for the
586 present purpose, and thus we used the brightness temperature difference to enhance
587 the dust signal for the LEB. No dust enhancement algorithm was applied to the
588 satellite data for the CD, which meant that the highest spatial resolution MODIS data
589 (0.25 x 0.25 km) could be used.

590

591 For the SAH, dust events during the four months April-July 2003 (which are typically
592 the months of greatest dust emission: *Goudie and Middleton*, [2001]) were identified
593 using MODIS (Terra) in the western half of the Sahara (west of 17°E). The satellite
594 data were enhanced using *Miller's* [2003] technique for dust enhancement (Table 4)
595 and all visible plumes were traced to identify the upwind source positions. Landsat
596 TM imagery, other satellite data and secondary sources were then used to classify
597 the land surface at the dust source to one of the geomorphic types in our scheme.
598 Some of the western Saharan dust plumes were traced to areas of complex
599 geomorphology where it was difficult to identify the dominant surface type or to areas
600 associated with human activity. However, these sources accounted for <5% of the
601 observed plumes.

602

603 <Table 4>

604

605 The use of satellite data to identify dust plumes and meteorological data to trace the
606 plume to its origin is relatively standard, but has some limitations (see e.g.
607 discussions by *Bullard et al.*, [2008]; *Lee et al.*, [2009]; *Baddock et al.* [2009]). First,
608 since many dust sources are not true 'points' but cover small areas, the allocation to
609 a single upwind point source is somewhat subjective. Dust can occur as a single
610 coherent plume or multiple dispersed plumes which means that even for a single
611 plume more than one dust source may be identified (Table 4; *Walker et al.* [2009]).
612 Additionally, the source points of some plumes may actually have been located a
613 short distance upwind of the point at which they become visible from MODIS
614 (depending on the relative timing of the dust emissions and the satellite overpass,
615 and surface wind speed). Second, this method does not consider the size or
616 concentration of the dust plume and the relative intensity (magnitude) of erosion at
617 each point is unknown. Thus, the data can only be used to evaluate

618 presence/absence of dust emission from specific geomorphic types. Third, visibility
619 measurements at meteorological stations tend to underestimate dust-event
620 frequency due to the low density of stations in most arid regions but MODIS may also
621 fail to capture dust events e.g. due to cloud cover or because of the relative timing of
622 dust events and MODIS data capture times (e.g. events occurring at night or
623 between satellite passes). Large and dense dust events, themselves, also tend to
624 obscure the identification of additional active dust sources on MODIS images which
625 produces a bias in favor of consistently upwind sources. Finally, over bright desert
626 surfaces some upwind plume edges can be hard to detect using MODIS, but use of
627 Level 1 band data from this sensor has been demonstrated more effective than
628 MODIS products (Level 2) such as Deep Blue for highest resolution of source pin-
629 pointing [Baddock *et al.*, 2009]. Despite these issues, the approach yields sufficiently
630 good results to allow testing of the proposed scheme.

631

632 **5. Evaluation of the Dust Source Scheme**

633 The aim of this project is to develop a theoretical classification of different types of
634 geomorphological surface with respect to their potential as dust sources. The
635 intention is that the classification can be applied globally and consequently can be
636 used to inform the surface characteristic parameters of global dust models used for
637 understanding dust emissions in the past, present and future. The maps and dust
638 point source data described above were therefore used to evaluate how workable the
639 proposed geomorphic scheme is in four different locations.

640

641 **5.1 Spatial Patterns**

642 It was possible to identify all seven basic geomorphic types across the CD, LEB and
643 the TAK (Figure 2). Some sub-types are not represented in particular regions, for
644 example there are no examples of loess in the CD. However, there were no surface
645 types that could not be classified using the proposed scheme i.e. all geomorphic
646 types present in these three regions are included within our theoretically-based
647 classification.

648 The use of a common scheme across the three regions makes it possible to compare
649 the relative spatial importance of each geomorphic type: this revealed considerable
650 differences among the regions. For example, aeolian sand deposits are more

651 extensive in the TAK (ca. 55% of total area) and LEB (ca. 39%) than in the CD (ca.
652 5%), while high relief alluvial systems are more important in the CD (ca. 43%) than in
653 the LEB (3%). Ephemeral lakes cover 4% of the CD and LEB and 7% of the TAK
654 (Table 5). Specific geomorphology can also vary within classes: the alluvial low relief
655 areas in CD are chiefly floodplains and deltas, for example, whereas in the LEB this
656 category encompasses anastomosing rivers with very wide floodplains.

657

658 <Figure 2>

659

660 Studies in different regions have shown that areas of common superficial
661 geomorphology do not necessarily behave in the same way (see section 2.1), and
662 accordingly, the number of dust plumes associated with each geomorphic class was
663 found to vary among the regions. Ephemeral and dry lakes (1b + 1d) account for a
664 large number of dust plumes – 66% in the SAH, 48% in the CD, 11% in the LEB
665 (Figure 3, Table 5). Sand sheets [5a] account for nearly 2%, 6% and 2% of dust
666 plumes in CD, LEB and SAH respectively. Sand dunes [5b] are relatively unimportant
667 in the CD (14%) and SAH (2%) compared with the LEB where they account for
668 around 60% of dust plumes. In the CD, 21% of dust plumes are from high relief,
669 unarmoured, unincised alluvial systems (2d). Across the CD, LEB and SAH, the most
670 significant alluvial surface for dust emissions was low relief, unarmoured and
671 unincised (3d): accounting for 12%, 16.5% and 25% of dust plumes respectively.
672 Less than 1% of alluvial dust sources in the LEB are armoured and unincised. Stony
673 surfaces [4] had low emissions in all three regions and there are no dust emissions
674 from perennial lakes [1a]. Although we have no comparable point source data for the
675 TAK, meteorological stations within and downwind (southwest) of the dunefield record
676 more dust events, particularly sand-dust storms than those to the north and east [*Ma*
677 *et al.*, 2006] and are typically associated with unarmoured alluvial deposits (3d).
678 Differences in emission from different geomorphic types may, of course, reflect
679 variability associated with different wind regimes in each region. Nevertheless, these
680 first-order comparisons show that emissions from many geomorphic types are
681 negligible (e.g. perennial lakes, stony surfaces, armoured alluvial systems, sand
682 sheets), and confirm the role of ephemeral lakes, unconsolidated and unarmoured
683 surfaces, and unincised surfaces as major contributors to regional dust fluxes.

684

685 <Table 5>

686 <Figure 3>

687

688 The use of percentage frequency of emissions as a tool for evaluating the
689 applicability of our geomorphic scheme to determine contribution to regional dust
690 emissions is complicated by differences in the area covered by different geomorphic
691 types in each region. To permit a more robust evaluation, we have calculated the
692 number of plumes per km² from each geomorphic type in the CD and LEB (Table 5).
693 In the CD, the most extensive geomorphic class is high relief alluvial, unarmoured
694 and unincised (nearly 43% of the area) but the number of plumes per km² on this
695 surface is 0.0003. There are over 20 times more dust plumes per km² from
696 ephemeral lakes (0.0072) which cover only 3% of the region. Although the number
697 of dust plumes per km² in the CD is similar for both ephemeral lakes (0.0072) and
698 stony surfaces (0.0071) this comparison is somewhat misleading; only one dust
699 plume was observed coming from a stony surface in the CD and a very small area of
700 the desert is characterized by this surface type (141 km², or <0.0005% total area).
701 Although sand dunes account for over 57% of dust plumes in the LEB, the number of
702 plumes per km² is only 0.001. The number of plumes per km² is slightly higher for
703 ephemeral lakes (0.0013) which cover less than 4% of the area and account for 11%
704 of the dust plumes. Unarmoured, unincised low relief systems [3d] produce similar
705 numbers of plumes per km² in the two regions, as do low-emission surfaces (Table
706 5). The most pronounced differences, in terms of plumes per km², between the CD
707 and LEB is for sand dunes and ephemeral lakes. There are twice as many dust
708 plumes from sand dunes in the LEB as in the CD, presumably reflecting the
709 differences in the history and activity status of the dunes. There are about three times
710 as many plumes from ephemeral lakes in the CD as in the LEB, again presumably
711 reflecting differences in the hydrology, chemistry and/or sedimentology of these
712 lakes. Nevertheless, the general pattern of relative importance of geomorphic types
713 as dust sources is consistent with our conceptual scheme as is the variability within
714 any geomorphic type.

715 Antecedent history and local factors clearly influence the amount of dust deflated
716 from specific geomorphic types, such that quantitative comparisons in terms of
717 plumes per km² tend to emphasize the differences between different regions. In order
718 to assess the usefulness of the proposed geomorphological classification of potential
719 sources at a more globally-applicable scale, we have therefore grouped the different

720 geomorphic types which, on theoretical grounds, are high, medium and low emitters
721 (column 5, Table 2) and then compared the regional emissions from these three
722 groups. In the CD, 48% of dust point sources are located in geomorphic types that
723 are predicted to have high emissions, 48% in areas of medium emissions and 4% in
724 areas of predicted low emissions. For the LEB, 11% of dust point sources are from
725 areas of high emissions, 80% of emissions are from areas of medium emissions, and
726 9% from areas predicted to have low emissions. The major source of uncertainty
727 here is the classification of sand dunes, which may either be low emitters (when they
728 are young and/or active) or high emitters (when they are old and/or stabilised and
729 have undergone recent disturbance).

730

731 **5.2 Temporal Variability**

732 We have not attempted to evaluate how well our scheme predicts temporal variability
733 in emissions because the available dust plume records from each region cover such
734 short periods of time (from 4 months to ten years). However, the data from the CD
735 and LEB do show considerable inter-annual variability in emissions from some
736 geomorphic types (Figure 4). Furthermore, variability in the activity of source surface
737 may largely be driven by interannual variability in wind regime.

738

739 Severe drought between 2001-2004 reduced vegetation cover in the CD, and as a
740 result, availability-limited alluvial surfaces were important emitters during this interval,
741 and particularly in 2001 [*Rivera Rivera et al.*, 2009]. The strong summer monsoon in
742 2006 caused the filling of many ephemeral lakes and re-vegetation of lake margins
743 and other surfaces, converting many areas from supply-limited to availability-limited
744 systems, and increasing the transport capacity required to entrain dust. As a result,
745 there was a significant decrease in the number of dust events in CD in 2006 and no
746 dust plumes were observed in 2007.

747 The high emissions from aeolian deposits in 2003 in the LEB are attributed to the
748 destabilising effect of fires on vegetation cover in the Simpson Desert in the previous
749 year [*Bullard, et al.*, 2008]. Different geomorphic types within the LEB are known to
750 respond in different ways to precipitation or drought [*McTainsh et al.*, 1999]. The
751 increase in emissions from supply-limited alluvial sources in 2005/6 is attributed to
752 flood events that occurred within the basin in January-March 2004, transporting new
753 sediment supplies to the lower basin [*Bullard et al.*, 2008].

754

755 <Figure 4>

756

757 **6. Implementation of Geomorphologically-controlled Sources in a** 758 **Modeling Context**

759

760 The desire to prescribe “preferential” dust-emission sources, rather than using
761 empirical information such as surface reflectance or surface roughness to capture the
762 spatial variability in emissions, arises from the need to predict (or retrodict) the
763 impacts of climate change on the dust cycle and the inadequacies of current global
764 data sets of soil and land-surface properties. Modeling schemes which specify
765 “preferential” dust-emission sources, such as topographic depressions or dry lake
766 beds, generally use this information to modify the textural properties of the soil in a
767 given source area to ensure it is highly susceptible to wind erosion, either explicitly
768 by increasing the amount of silt-sized material present or implicitly by increasing the
769 simulated emissions by some arbitrary factor (see e.g. *Tegen et al.* [2002]). Current
770 approaches have been limited both in terms of the number of types of “preferential”
771 sources they recognise, and because these sources have been mapped and applied
772 at the spatial scale of the model (e.g. over a whole e.g. 0.5 x 0.5° grid cell). Our
773 scheme characterizes the land-surface into a set of geomorphic types with different
774 emission potentials (from non-emitters, through low emitters to high emitters) and
775 recognises that, even under ideal meteorological conditions for dust deflation, each
776 type can have a different temporal behaviour (from continuous emitters to sporadic
777 emitters) depending on the degree to which they are sediment-limited. The scheme
778 could be applied at a range of spatial scales: in the examples used here as test
779 regions, we have mapped the different geomorphic types at 1 km resolution,
780 sufficient to be able to calculate the varying proportions of each type with a 0.5 x 0.5°
781 grid cell typical of the resolution of many dust-cycle models. There is a considerable
782 amount of work to be done to provide a global map of geomorphic types using the
783 current scheme. Nevertheless, such a map in combination with existing global soils
784 data would be an invaluable tool to improve the modeling both of the spatial and
785 temporal variability of emissions

786

787 Our scheme provides a way of distinguishing emitting and basically non-emitting
788 surfaces within potential dust source areas. The scheme could therefore be used to

789 derive an estimation of the percentage of each of geomorphic subtype within a model
790 grid-cell (see e.g. Figure 5a, b). At its simplest, the scheme provides a means to
791 reduce emissions from individual model grid-cells by reducing simulated dust flux
792 according to how much of a grid-cell is non-emitting, or only likely to emit
793 intermittently. Furthermore, we have shown that the scheme can be used to sub-
794 divide geomorphic types in a qualitative sense into low, medium and high emitters
795 (Figure 5c, d, e), thus allowing simulated emissions to be tuned accordingly.
796 Although the influence of antecedent conditions and local geomorphic factors makes
797 the division into low, medium and high emitters more prone to error (unless guided by
798 local information), this division would allow further tuning of model emissions and can
799 be applied at a range of scales (Figure 6).

800

801 <Figure 5>

802 <Figure 6>

803

804 The scheme also provides information on the presence and relative importance of
805 geomorphic types that are sediment supply-limited and the nature of the pre-
806 conditioning that transforms these areas from non-emitters to emitters. Our data from
807 the western Sahara (April-July 2003) do not include any dust emissions associated
808 with high relief alluvial systems such as alluvial fans, however *Schepanski et al.*
809 [2007] did identify alluvial fans as a potential Saharan dust source during June-
810 August 2006. Although neither data set is long enough to test this conclusively, this
811 is likely to be an example of the temporary transformation of a non-emitting surface
812 to an emitting surface, and we have demonstrated similar behavior in longer records
813 from the CD and LEB (Section 5.2). In a modeling context, it would be inappropriate
814 to consider sediment-supply limited geomorphic types (such as alluvial fans) as
815 major emitters because they do not emit on a regular basis but only for short and/or
816 infrequent intervals as a result of specific pre-conditioning which provides readily
817 erodible material. In regions where sediment supply to such geomorphic types is
818 increased through sporadic flooding or through fluvial erosion, it should be possible
819 to use information about recent and contemporary climate conditions to determine
820 when these sources are likely to become dust sources. For example, an extremely
821 wet season/year could be identified as a trigger for emissions in the subsequent
822 season/year in sediment-supply limited geomorphic types [*McTainsh et al.*, 1999;

823 *Reheis and Kihl, 1995*]. Incorporating such “transformations” in dust-cycle models
824 could go some way to improving the simulation of inter-annual variability of dust
825 emission, one of the most complex aspects of source behaviour.

826

827 The presence of a sand source (i.e. a source of coarse saltators) is the primary
828 determinant of whether predominantly fine-grained materials (e.g. lake deposits) are
829 an emission source or not. Surface mapping provides pertinent information on
830 geomorphic adjacency, and thus can be used to determine sand availability upwind
831 of an area of fine-grained material. Given that sandblasting is explicitly incorporated
832 in many models, this information can be used as a switch: where sand is available
833 upwind, areas of predominantly fine-grained material (e.g. lake beds) could be
834 considered dust sources; where sand is not available upwind, they might not.
835 Implementing this within a modeling framework requires two factors to be
836 determined. The first is the distance threshold for adjacency. A sand source adjacent
837 to a lake bed may act as a source of coarse saltators and lead to emissions but, if the
838 lake deposits cover a considerable area, these emissions will be confined to the part
839 of the lake closest to the sand source [*Cahill et al., 1996; Bullard et al., 2008*]. There
840 will be no emissions in more distant parts of the lake bed. The distance threshold for
841 adjacency is clearly dependent on wind speed and sand size, and thus would need to
842 be calculated interactively by the model. The second factor that needs to be taken
843 into account is the impact of changes in wind direction, since sand sources may be
844 highly localised. Given the relatively coarse resolution of most dust-cycle models,
845 changes in wind direction are unlikely to be sufficiently large under modern
846 conditions to have an impact on sand-source adjacency but this is a factor that would
847 need to be considered in running simulations under radically different climate forcings
848 e.g. the last glacial maximum.

849

850 **7. Discussion and Future Perspectives**

851 We have developed a simple classification of geomorphic types related to their
852 behaviour as dust sources, based on current understanding of the geomorphological
853 controls on dust emissions. We have demonstrated that the scheme can be applied
854 to four major dust source regions, primarily using remote-sensing imagery to classify
855 surfaces, and thus is suitable for global application. We have shown that the scheme
856 is useful in predicting areas of high or low emission, and that it also provides a

857 framework for understanding the temporal behaviour of intermittent emitters. Finally,
858 we have indicated ways in which elements of this scheme could be incorporated into
859 dust-cycle models in order to improve the simulations of preferential sources and the
860 interannual variability of emissions. Although much of the detailed geomorphological
861 information available in regional maps is lost, this simplified scheme incorporates far
862 more complexity than is typically present in global dust models and effectively
863 represents the geomorphic reality (albeit qualitatively) of dust emission processes
864 and controlling factors.

865 We have demonstrated that our geomorphic scheme can be applied in four different
866 locations. Although for the most part this was achieved using satellite data and
867 secondary sources, field experience was particularly helpful in determining, for
868 example, the difference between armoured and unarmoured surfaces. Mapping of
869 landforms from aerial photographs or remotely sensed images has a long history
870 and, when combined with field knowledge of a region, can provide detailed
871 information (as shown here) that could not be generated using an automated pattern-
872 recognition algorithm. The mapping scheme now needs to be tested in other regions,
873 and particularly in regions where geomorphic surface sub-types that are not present
874 in our test regions occur (see Table 2). It may be necessary to expand the
875 classification in order to apply it globally. For example, the scheme does not currently
876 include anthropogenically-modified surfaces, such as agricultural or urban areas, all
877 of which have been identified as dust sources in the Sahara-Sahel [*Ginoux et al.*,
878 2010; *Ladji et al.*, 2010], southwestern North America [*Lee et al.*, 2009] and parts of
879 China [*Wang et al.*, 2006]. Nevertheless, we believe the framework presented here
880 provides a good basis for the development of a global map of dust sources and could
881 be applied with only minor modification in other areas.

882 We have shown that some surface geomorphologies (e.g. ephemeral lakes and
883 alluvial sources) are highly variable with respect to emission potential. In global
884 terms, dunefields are not a significant source of dust: in the western Sahara <2% of
885 dust plumes originate from dunefields and only 8% of plumes in the CD originate
886 from dunes. However, in the LEB 60% of the observed plumes originated from
887 dunefields. These differences probably reflect differences in dune type (i.e. migrating
888 versus stable dunes), age (young versus old), sedimentology and climate (i.e. hyper-
889 arid versus semi-arid). The contrast between dunefield emissions in the SAH and
890 LEB, for example, appears to reflect the palaeoenvironmental history of the regions;
891 the Saharan dunes have been reworked following successive glacial cycles whereas
892 the dunes in the LEB have been stable for a longer period and hence accumulated

893 more fine material [*Lancaster et al.*, 2002; *Muhs*, 2004; *Hesse*, 2010; *Strong et al.*,
894 2010]. Subdividing the aeolian dune class [5b] according to dune type, activity and
895 palaeo-history could certainly improve the current classification scheme but would be
896 a significant task involving more extensive use of field studies.

897 There is also considerable variability in emissions from exposed lake beds. To some
898 extent, this may reflect the availability of coarse saltators and hence the degree of
899 connectivity between this geomorphic type and types that are sources of sand-sized
900 material. The current scheme provides a mechanism for taking adjacency of different
901 geomorphic types into account in the prediction of emissions. However, the variability
902 in emissions from exposed lake beds also reflects the interplay between surface
903 properties and palaeoenvironmental history, in particular as it determines lake
904 hydrogeochemistry and hence the precipitation of different types of salts as well as
905 crust strengths [*Reynolds et al.*, 2007]. This can vary even within a single playa [e.g.
906 *Gillette et al.*, 2001] or throughout a source region as a whole. For example, in the
907 LEB, Lake Eyre North is a major dust source while Lake Frome is not, because of the
908 presence of surface salts on the latter. Remote sensing has been used to
909 discriminate different types of salt deposits [e.g. *Crowley and Hook*, 1996; *Drake*
910 1995; *Drake et al.*, 1994; *Katra and Lancaster*, 1998] and thus it should be possible
911 to extend the current classification to take this factor into account in mapping
912 ephemeral lake types. We would strongly argue for the need to test such a sub-
913 division of ephemeral lakes against dust plume data in order to facilitate an extension
914 of the current scheme.

915 Reliance on remote-sensing observations is necessary if the current scheme is to be
916 applied globally. However, scale is a major issue in mapping the occurrence of
917 specific geomorphic types and also affects our ability to test the relationship between
918 these geomorphic types and dust emissions. Many potential dust sources (e.g.
919 interdunal depressions) are small, and the existence of fine-scale mosaics of different
920 geomorphic types may make the differentiation of dust sources difficult. Scale issues
921 may have introduced considerable noise into our assessment of the relationships
922 between geomorphic types and dust emissions. In the CD dataset, for example, 30
923 dust plumes were identified as originating from sand dunes in the area around White
924 Sands and Palaeolake Palomas. Of these 11 were located within 2 km of a dry lake,
925 a further 11 were located 2-5 km from a dry lake and 8 were located more than 5 km
926 away. Given the resolution of the mapping and satellite data used (≤ 1 km) it is highly
927 likely that some of the emission that we have attributed to dune sources closest to
928 the lake may in fact have been from the lake surface or a direct result of interaction

929 between the dunes and the lake sediments [*Cahill et al.*, 1996; *Lee et al.*, 2009;
930 *Baddock et al.*, 2011].

931 Despite these various caveats, the scheme proposed here provides a way of
932 improving the current prescription of preferential sources in dust-cycle models. It
933 allows improved delineation of emitting and non-emitting surfaces, provides a guide
934 to surface texture of these features that could be used to modify standard soils input
935 data sets, and indicates how the temporal behavior of potential sources can be
936 considered in terms of climatic thresholds. We believe that implementing this kind of
937 process-informed scheme within a global-modeling framework will considerably
938 improve our ability to simulate dust emissions in response to climate change.
939 However, there are a number of steps required before it is feasible to implement the
940 proposed scheme globally. These are:

941 1) to expand the evaluation of the current scheme within the four major source
942 regions examined here. In part, this requires additional work to make it possible to
943 apply the same evaluation approach for all regions, by e.g. extending the mapping of
944 the SAH and developing a dust point source data set for the TAK. However,
945 additional tests of the scheme could be possible, for example by (a) extending the
946 period for which point data is available for the LEB and SAH to cover the most recent
947 years, (b) exploring the use of soils data (both local and global data sets) to improve
948 the mapping of surface characteristics, and (c) utilizing (or in some cases
949 implementing) ground-based measurements of dust emission from different dust
950 source types;

951 2) to test the applicability of the current scheme in other dust source regions.
952 Key questions here include (a) whether it is necessary to expand the scheme to
953 include e.g. anthropogenically-modified surfaces; (b) whether it is feasible to use
954 remote-sensing products to differentiate different types of salt crusts which influence
955 erodibility of dry lakes; and (c) whether it is feasible to use field studies of
956 geomorphic history to differentiate between dune types of different ages. Determining
957 whether these modifications are necessary and helpful will in large part be
958 determined by whether the modification is likely to affect a large area in global terms
959 and whether the new categories can be mapped consistently from region to region;

960 3) to implement the scheme globally to provide a single gridded map of dust
961 source characteristics as an input field for modeling. One possible way forward here
962 is to use existing base maps (e.g. *Hesse*, 2010) or ongoing mapping projects (e.g.
963 Sand Seas and Dune Fields of the World:

964 <http://inquadunesatlas.dri.edu/background.htm>) as an initial basis for mapping dust
965 source areas;

966 4) to develop quantified relationships from well-studied regions between land
967 surface types and dust fluxes, focusing specifically on active area, seasonal timing,
968 and interannual variability.

969

970 While there is still work to do to refine and test the proposed scheme, the real test of
971 the usefulness of this classification will only come when it is implemented within a
972 dust-cycle model. Initially, this can only be done for the three regions we have
973 already mapped. However, these regions represent significant dust sources under
974 current conditions and encompass a sufficient range of surface types and temporal
975 behaviors to make a model-based evaluation worthwhile.

976

977

978

979

980

981

982 **Acknowledgements**

983 This paper was conceived and developed at two meetings of the QUEST Working
984 Group on Dust (Exeter 2007, Villefranche-sur-Mer 2008). We thank the QUEST
985 programme for providing funding for these workshops. This paper is a contribution to
986 the QUEST DESIRE project (SPH) and to INQUA Project 0802. TG was supported
987 from the Texas Advanced Research Program under Grant No. 3661-0027-2007 and
988 NOAA through the Educational Partnership Program for Minority Serving Institutions
989 (EPP/MSI) Cooperative Agreement NA17AE1623.

990

991

992

993 **References**

- 994 Ackerman, S. A. (1997), Remote sensing aerosols using satellite infrared
995 observations, *J. Geophys. Res.*, 102(D14), 17069-17079.
- 996 Adelsberger, K.A., and J. R. Smith (2009), Desert pavement development and
997 landscape stability on the Eastern Libyan Plateau, Egypt. *Geomorphology*,
998 107(3-4), 178-194.
- 999 Alfaro, S. C., and L. Gomes (2001), Modeling mineral aerosol production by wind
1000 erosion: emission intensities and aerosol size distributions in source areas, *J.*
1001 *Geophys. Res.*, 106(D16), 18075-18084.
- 1002 Ashley, W. S., and A. W. Black (2008), Fatalities associated with nonconvective high
1003 wind events in the United States, *J. App. Met. Clim.*, 47(2), 717-725.
- 1004 Baddock, M. C., J. E. Bullard, and R. G. Bryant (2009), Dust source identification
1005 using MODIS: a comparison of techniques applied to the Lake Eyre Basin,
1006 Australia, *Remote Sens. Environ.*, 113(7), 1511-1528.
- 1007 Baddock, M. C., T. E. Gill, J. E. Bullard, M. Dominguez Acosta, and N. I. Rivera
1008 Rivera (2011), A geomorphic map of the Chihuahuan Desert, North America,
1009 based on potential dust emissions, *J. Maps*, 2011, 249-259.
- 1010 Ballantine, J-A., G. S. Okin, D. E. Prentiss, and D. A. Roberts (2005), Mapping north
1011 African landforms using continental scale unmixing of MODIS imagery,
1012 *Remote Sens. Environ.*, 97, 470-483.
- 1013 Bessagnet, B., L. Menut, G. Aymoz, H. Chepfer, and R. Vautard (2008), Modeling
1014 dust emissions and transport within Europe: the Ukraine March 2007 event, *J.*
1015 *Geophys. Res.*, 113(D15), D15202.
- 1016 Belnap, J., and S. D. Warren (2002), Patton's tracks in the Mojave Desert, USA: an
1017 ecological legacy, *Arid Land Res. Manag.*, 16, 245-258.
- 1018 Bullard, J. E., and M. J. Austin (2011), Dust generation on a proglacial floodplain,
1019 West Greenland, *Aeolian Research*, 3, 43-54.
- 1020 Bullard, J. E., and G. H. McTainsh (2003), Aeolian-fluvial interactions in dryland
1021 environments: scales, concepts and Australia case study, *Prog. Phys. Geog.*,
1022 27, 471-501.
- 1023 Bullard, J. E., and K. H. White (2005), Dust production and the release of iron oxides
1024 resulting from the aeolian abrasion of natural dune sands, *Earth Surf. Proc.*
1025 *Landf.*, 30, 95-106.

- 1026 Bullard, J. E., G. H. McTainsh, and C. Pudmenzky (2007), Factors affecting the
1027 nature and rate of dust production from natural dune sands, *Sedimentology*,
1028 54(1), 169-182.
- 1029 Bullard, J. M. Baddock, G. McTainsh, and J. Leys (2008), Sub-basin scale dust
1030 source geomorphology detected using MODIS, *Geophys. Res. Lett.*, 35(15),
1031 L15404, doi:2008GL033928.
- 1032 Cahill, T. A., T. E. Gill, J. E. Reid, E. A. Gearhart, and D. A. Gillette (1996), Saltating
1033 particles, playa crusts and dust aerosols from Owens (Dry) Lake, California,
1034 *Earth Surf. Proc. Landf.*, 21, 621-639.
- 1035 Callot, Y., B. Marticorena, and G. Bergametti, G. (2000), Geomorphologic approach
1036 for modelling the surface features of arid environments in a model of dust
1037 emissions: application to the Sahara desert, *Geodinamica Acta*, 13, 245-270.
- 1038 Chatenet, B., B. Marticorena, L. Gomes, and G. Bergametti (1996), Assessing the
1039 microped size distributions of desert soils erodible by wind, *Sedimentology*,
1040 43(5), 901-911.
- 1041 Cooke, R. U. (1970), Stone pavements in deserts, *Ann. Am. Ass. Geogr.* 60, 560-
1042 577.
- 1043 Crouvi, O., R. Amit, Y. Enzel, N. Porat, and A. Sandler (2008), Sand dunes as a
1044 major proximal dust source for late Pleistocene loess in the Negev Desert,
1045 Israel, *Quat. Res.*, 70, 275-282.
- 1046 Crowley, J. K., and S. J. Hook (1996). Mapping playa evaporite minerals and
1047 associated sediments in Death Valley, California, with multispectral thermal
1048 infrared images, *J. Geophys. Res.*, 101(B1), 643-660.
- 1049 de Baar, H.J.W. et al. (2005), Synthesis of iron fertilization experiments: from the Iron
1050 Age in the Age of Enlightenment, *J. Geophys. Res.*, 110(C9), C09S16.
- 1051 Dentener, F.J., G. R. Carmichael, Y. Zhang, J. Lelieveld, and P. J. Crutzen (1996),
1052 Role of mineral aerosol as a reactive surface in the global troposphere, *J.*
1053 *Geophys. Res.*, 101, 22869-22889.
- 1054 Derbyshire, E., X. Meng, and R. A. Kemp (1998), Provenance, transport and
1055 characteristics of modern aeolian dust in western Gansu Province, China, and
1056 interpretation of the Quaternary loess record, *J. Arid Environ.*, 39, 497-516.

- 1057 Desboeufs, K.V., A. Sofikitis, R. Losno, J. L. Colin, and P. Ausset (2005), Dissolution
1058 and solubility of trace metals from natural and anthropogenic particulate
1059 matter, *Chemosphere*, 58(2), 195-203.
- 1060 Drake, N. A. (1995), Reflectance spectra of evaporite minerals (400-2500 nm):
1061 applications for remote sensing, *Int. J. Remote Sensing*, 16, 2255-2572.
- 1062 Drake, N.A., and R. G. Bryant (1994), Monitoring the flooding ratio of Tunisian playas
1063 using AVHRR imagery and its potential for evaluating changes in playa
1064 hydrology, geomorphology and biota, in *Environmental Change in Drylands*
1065 edited by A.C. Millington and K. Pye, pp. 347-364, Wiley, Chichester.
- 1066 Drake, N.A., R. Handley, T. O'Loingsigh, N. Brooks, and R. Bryant (2008), Identifying
1067 Saharan dust sources using remote sensing: a comparison of TOMS AI,
1068 Meteosat IDDI and a new MODIS Dust Index. *Geophysical Research*
1069 *Abstracts*, 10, EGU2008-A-11858.
- 1070 Durant, A. J., S. P. Harrison, I. M. Watson, and Y. Balkanski (2009), Sensitivity of
1071 direct radiative forcing by mineral dust to particle characteristics, *Prog. Phys.*
1072 *Geog.*, 33(1), 80-102.
- 1073 Foltz, G.R., and M. J. McPhaden (2008), Impact of Saharan dust on tropical North
1074 Atlantic SST, *J. Climate*, 21, 5048-5060.
- 1075 Forster, P. et al. (2007), Changes in Atmospheric Constituents and in Radiative
1076 Forcing, in *Climate Change 2007; The Physical Science Basis. Contribution*
1077 *of Working Group I to the Fourth Assessment Report of the Intergovernmental*
1078 *Panel on Climate Change* edited by S. Solomon, D. Qin, M. Manning, Z.
1079 Chen, M. Marquis, K. B. Averyt, M. Tignor, M. and H. L. Miller, Cambridge
1080 University Press, Cambridge, UK and New York, NY, USA.
- 1081 Geosciences Australia (2008), *NATMAP Digital Maps 250K*. Geoscience Australia,
1082 Australian Government, Canberra.
- 1083 Gill, T.E. (1996), Eolian sediments generated by anthropogenic disturbance of
1084 playas: human impacts on the geomorphic system and geomorphic impacts
1085 on the human system, *Geomorphology*, 17(1-3), 207-228.
- 1086 Gillette, D.A., D.W. Fryrear, T.E. Gill, T. Ley, T.A. Cahill, and E. A. Gearhart (1997),
1087 Relation of vertical flux of particles smaller than 10 μ m to total aeolian
1088 horizontal mass flux at Owens lake. *J. Geophys. Res.*, 102(D22), 26009-
1089 26015.

- 1090 Gillette, D.A. (1999), A qualitative geophysical explanation for hot spot dust emitting
1091 source regions, *Contributions to Atmospheric Physics*, 72(1), 67-77.
- 1092 Gillette, D.A., and W. A. Chen (2001), Particle production and aeolian transport from
1093 a "supply limited" source area in the Chihuahuan Desert, New Mexico, United
1094 States, *J. Geophys. Res.*, 106(D6), 5267-5278.
- 1095 Gillette, D.A., T.C. Niemeier, and P.J. Helm (2001), Supply-limited horizontal sand
1096 drift at an ephemerally crusted, unvegetated saline playa, *J. Geophys. Res.*,
1097 106(D16), 18085-18098.
- 1098 Ginoux, P., M. Chin, I. Tegen, J. M. Prospero, B. N. Holben, O. Dubovik, and S.-J.
1099 Lin (2001), Sources and distribution of dust aerosols with the GOCART
1100 model, *J. Geophys. Res.*, 106(D17), 20255-20273.
- 1101 Ginoux, P., D. Garbuzov, and N.C. Hsu (2010), Identification of anthropogenic and
1102 natural dust sources using Moderate Resolution Imaging Spectroradiometer
1103 (MODIS) Deep Blue level 2 data, *J. Geophys. Res.*, 115, D05204,
1104 doi:10.1029/2009JD012398.
- 1105 Glennie, K.W. (1970), *Desert Sedimentary Environments*, Elsevier, New York.
- 1106 Gomes, L., G. Bergametti, G. Coudé-Gaussen, and P. Rognon (1990), Submicron
1107 desert dusts: a sandblasting process, *J. Geophys. Res.*, 95(D9), 13927-
1108 13935.
- 1109 Griffin, D. W., and C. A. Kellogg (2004), Dust storms and their impact on ocean and
1110 human health. Dust in Earth's Atmosphere. *Ecohealth* 1, 284-295.
- 1111 Grini, A., and C. S. Zender (2004), Roles of saltation, sandblasting and wind speed
1112 variability on mineral dust aerosol size distribution during the Puerto Rican
1113 Dust Experiment (PRIDE), *J. Geophys. Res.*, 109, D07202,
1114 doi:10.1029/2003JD004233.
- 1115 Grini, A., G. Myhre, C. S. Zender, and I. S. A. Isaksen, (2005), Model simulations of
1116 dust sources and transport in the global atmosphere: effects of soil erodibility
1117 and wind speed variability, *J. Geophys. Res.*, 110, D02205,
1118 doi:10.1029/2004JD005037.
- 1119 Handford, C.R. (2006), Sedimentology and evaporite genesis in a Holocene
1120 continental-sabkha playa basin - Bristol Dry Lake, California, *Sedimentology*,
1121 29, 239-253.

- 1122 Haywood, J., and O. Boucher (2000), Estimates of the direct and indirect radiative
1123 forcing due to tropospheric aerosols: a review, *Rev. Geophys.*, 38(4), 513-
1124 543.
- 1125 Hesse, P. (2010), The Australian desert dunefields: formation and evolution in an old,
1126 flat, dry continent, region, in *Australian Landscapes* edited by P. Bishop and
1127 B. Pillans, Special Publication 346, 141-164, Geological Society, London.
- 1128 INEGI (Instituto Nacional de Estadística, Geografía y Informática, México) (2001),
1129 Sistema de Topoformas. Available online at
1130 [http://mapserver.inegi.org.mx/geografia/espanol/prodyserv/iris/html/informacio](http://mapserver.inegi.org.mx/geografia/espanol/prodyserv/iris/html/informacionespecializada/proy fisiografia.cfm)
1131 [n especializada/proy fisiografia.cfm](http://mapserver.inegi.org.mx/geografia/espanol/prodyserv/iris/html/informacionespecializada/proy fisiografia.cfm) Accessed 31/08/2010.
- 1132 IUSS Working Group WRB. 2007. World Reference Base for Soil Resources 2006,
1133 first update 2007. *World Soil Resources Reports* No. 103. FAO, Rome.
- 1134 Jickells, T.D. et al. (2005), Global iron connections between desert dust, ocean
1135 biogeochemistry and climate, *Science*, 308, 67-71.
- 1136 Karam, D.B., C. Flamant, P. Tulet, M. C. Todd, J. Pelon, and E. Williams (2009), Dry
1137 cyclogenesis and dust mobilization in the intertropical discontinuity of the
1138 West African Monsoon: a case study, *J. Geophys. Res.*, 114, D05115.
- 1139 Ktra, I., and N. Lancaster (2008), Surface-sediment dynamics in a dust source from
1140 spaceborne multispectral thermal infrared data, *Remote Sens. Environ.*,
1141 112(7), 3212-3221.
- 1142 Kocurek, G. (1998), Aeolian system response to external forcing factors – a
1143 sequence stratigraphic view of the Saharan region, in *Quaternary Deserts*
1144 *and Climatic Change* edited by A. S. Alsharhan, K. W. Glennie, G. L. Whittle,
1145 and C. G. St.C. Kendall, C.G.St.C. pp. 327-349, Balkema, Rotterdam.
- 1146 Kocurek, G., and K. Havholm (1993), Aeolian sequence stratigraphy – a conceptual
1147 framework, in *Siliclastic Sequence Stratigraphy* edited by P. Weimer, and H.
1148 Posamentier, pp. 393-409, American Association of Petroleum Geologists,
1149 Memoir 58, Tulsa, Oklahoma.
- 1150 Koven, C.D., and I. Fung (2008), Identifying global dust source areas using high-
1151 resolution land surface form. *J. Geophys. Res.*, 113, D22204,
1152 doi:10.1029/2008JD010195.

- 1153 Krah, M., T.S. McCarthy, H. Annegarn, and L. Ramberg (2004), Airborne dust
1154 deposition in the Okavango delta, Botswana, and its impact on landforms,
1155 *Earth Surf. Proc. Landf.*, 29, 565-577.
- 1156 Ladji, R., N. Yassaa, C. Balducci, and A. Cecinato (2010), Organic component of
1157 Algerian desert dusts, *Chemosphere*, 81(7), 925-931.
- 1158 Lancaster, N. et al. (2002), Late Pleistocene and Holocene dune activity and wind
1159 regimes in the western Sahara of Mauritania, *Geology*, 30(11), 991-994.
- 1160 Lee, J.A., T. E. Gill, K. R. Mulligan, M. D. Acosta, and A. E. Perez (2009), Land
1161 use/land cover and point sources of the 15 December 2003 dust storm in
1162 southwestern North America, *Geomorphology*, 105, 18-27,
1163 doi:10.1016/j.geomorph.2007.12.016.
- 1164 Li, J., G. S. Okin, L. Alvarez, and H. Epstein (2007), Quantitative effects of vegetation
1165 cover on wind erosion and soil nutrient loss in a desert grassland of southern
1166 New Mexico, USA, *Biogeochemistry*, 85(3) 317-332.
- 1167 Ma, Y., K. T. Xiao, and X. Wang, (2006), Climatological characteristics of dust
1168 weathers in the Tarim Basin, *Acta Scientiarum Naturalium Universitatis*
1169 *Pekinensis*, 1(1), No: pkuxbw2006002.
- 1170 Mahowald, N., K. Kohfeld, M. Hansson, Y. Balkanski, S. P. Harrison, I. C. Prentice,
1171 M. Schulz, and H. Rodhe (1999), Dust sources and deposition during the last
1172 glacial maximum and current climate: a comparison of model results with
1173 paleodata from ice cores and marine sediments, *J. Geophys. Res.*, 104(D13),
1174 15895-15916.
- 1175 Mahowald, N. M., R. G. Bryant, J. del Corral, and L. Steinberger (2003), Ephemeral
1176 lakes and dust sources, *Geophys. Res. Lett.*, 30(2), art.no.1074.
- 1177 Mahowald, N. M., D. R. Muhs, S. Levis, P. J. Rasch, M. Yoshioka, C. S. Zender, and
1178 C. Luo (2006), Change in atmospheric mineral aerosols in response to
1179 climate: last glacial period, preindustrial, modern and doubled carbon dioxide
1180 climates, *J. Geophys. Res.*, 111, D10202, doi:10.1029/2005JD006653.
- 1181 Mahowald, N., J. A. Ballantine, J. Feddema, and N. Ramankutty (2007), Global
1182 trends in visibility: implications for dust sources, *Atmos. Chem. Phys.*, 7,
1183 3309-3339.

- 1184 Marticorena, B., G. Bergametti, B. Aumont, Y. Callot, C. NDoume, and M. Legrand
1185 (1997), Modeling the atmospheric dust cycle .2. simulation of Saharan dust
1186 sources, *J. Geophys. Res.*, 102(D4), 4387-4404.
- 1187 McFadden, L.D., S. G. Wells, and M. J. Jercinovich (1987), Influences of eolian and
1188 pedogenic processes on the origin and evolution of desert pavement,
1189 *Geology*, 15, 504-508.
- 1190 McGowan, H.A., and A. Clark, A. (2008), A vertical profile of PM10 dust
1191 concentrations measured during a regional dust event identified by MODIS
1192 Terra, western Queensland, Australia, *J. Geophys. Res.*, 113, F02S03,
1193 doi:10.1029/2007JF000765.
- 1194 McKenna-Neuman, C., and R. Gilbert (1986), Aeolian processes and landforms in
1195 glaciofluvial environments of southeastern Baffin Island, NWT, Canada, in
1196 *Aeolian Geomorphology* edited by W. G. Nickling, pp. 213-235, Allen &
1197 Unwin, Boston.
- 1198 McTainsh, G., and C. Strong (2007), The role of aeolian dust in ecosystems,
1199 *Geomorphology*, 89, 39-54.
- 1200 McTainsh, G.H., J. F. Leys, and W. G. Nickling (1999), Wind erodibility of arid lands
1201 in the Channel Country of western Queensland, Australia, *Z. Geomorphologie*
1202 *N.F.* 116, 113-130.
- 1203 Middleton, N. J., A. S. Goudie, and G. L. Wells (1986), The frequency and source
1204 areas of dust storms, in *Aeolian Geomorphology* edited by W. G. Nickling, pp.
1205 237-259, Allen & Unwin, Boston.
- 1206 Miller, S. D. (2003), A consolidated technique for enhancing desert dust storms with
1207 MODIS, *Geophys. Res. Lett.*, 30(20), ASC12-1-4.
- 1208 Muhs, D. R. (2004), Mineralogical maturity in dunefields of North America, Africa and
1209 Australia, *Geomorphology*, 59, 247-269.
- 1210 Muhs, D. R., T. A. Ager, J. Been, J. P. Bradbury, and W. E. Dean (2003), A late
1211 Quaternary record of eolian silt deposition in a maar lake, St Michael Island,
1212 western Alaska, *Quat. Res.*, 60, 110-122.
- 1213 Muhs, D. R., J. R. Budahn, J. M. Prospero, and S. N. Carey (2007). Geochemical
1214 evidence for African dust inputs to soils of western Atlantic islands: Barbados,
1215 the Bahamas and Florida, *J. Geophys. Res.*, 112,
1216 doi:10.1029/2005JF000445.

- 1217 Nickling, W.G. (1978). Eolian sediment transport during dust storms: Slims River
1218 Valley, Yukon Territory, *Can. J. Earth Sci.*, 15, 1069-1084.
- 1219 Okin, G.S. (2005), Dependence of wind erosion and dust emission on surface
1220 heterogeneity: stochastic modeling, *J. Geophys. Res.*, 110(D11), D11208.
- 1221 Pelletier, J. D., M. Cline, and S. B. DeLong (2007), Desert pavement dynamics:
1222 numerical modeling and field-based calibration, *Earth Surf. Proc. Landf.*,
1223 32(13), 1913-1927.
- 1224 Peterson, F. F. (1980), Holocene desert soil formation under sodium salt influence in
1225 a playa-margin environment, *Quat. Res.*, 13, 172-186.
- 1226 Prospero, J.M., P. Ginoux, O. Torres, S. E. Nicholson, and T. E. Gill (2002),
1227 Environmental characterization of global sources of atmospheric soil dust
1228 identified with the Nimbus 7 Total Ozone Mapping Spectrometer (TOMS)
1229 absorbing aerosol product, *Rev. Geophys.*, 40(1), art.no.1002.
- 1230 Raymond, O. L., and A. J. Retter (2010), *Surface geology of Australia* 1:1,000,000
1231 scale 2010 edition (editors) [digital dataset]. Geoscience Australia,
1232 Commonwealth of Australia, Canberra, <http://www.ga.gov.au>
- 1233 Reheis, M. (1997), Dust deposition downwind of Owens (dry) Lake, 1991-1994:
1234 preliminary findings, *J. Geophys. Res.*, 102(D22), 25999-26008.
- 1235 Reheis, M.C. (2006), A 16-year record of eolian dust in Southern Nevada and
1236 California, USA: controls on dust generation and accumulation, *J. Arid*
1237 *Environ.*, 67(3), 487-520.
- 1238 Reheis, M.C., and R. Kihl (1995), Dust deposition in southern Nevada and California,
1239 1984-1989: relations to climate, source area and source lithology, *J.*
1240 *Geophys. Res.*, 100(D5), 8893-8918.
- 1241 Reynolds, R., J. Neff, M. Reheis, and P. Lamothe (2006), Atmospheric dust in
1242 modern soil on aeolian sandstone, Colorado Plateau (USA): variation with
1243 landscape position and contribution to potential plant nutrients, *Geoderma*,
1244 130(1-2), 108-123.
- 1245 Reynolds, R. et al. (2007), Dust emission from wet and dry playas in the Mojave
1246 desert, USA, *Earth Surf. Proc. Landf.*, 32(12), 1811-1827.
- 1247 Ridgwell, A.J. (2002), Dust in the Earth system: the biogeochemical linking of land,
1248 air and sea, *Philos. T. R. Soc. Lond.*, A. 360(1801), 2905-2924.

- 1249 Rivera Rivera, N.I. et al. (2009), Wind modeling of Chihuahuan Desert dust
1250 outbreaks, *Atmos. Environ.*, 43, 347-354.
- 1251 Rojo, R., T. E. Gill, and D. A. Gillette (2008), Particle size/composition relationships
1252 of wind-eroding sediments, Owens (dry) Lake, California, USA, *X-Ray*
1253 *Spectrom.*, 37(2), 111-115.
- 1254 Rosenfeld, D., Y. Rudich, and R. Lahav (2001), Desert dust suppressing
1255 precipitation: a possible desertification feedback loop, *Proc. Nat. Acad. Sci.*
1256 *USA*, 98, 5975-5980.
- 1257 Schepanski, K., I. Tegen, B. Laurent, B. Heinold, and A. Macke (2007), A new
1258 Saharan dust source activation frequency map derived from MSG-SEVIRI IR-
1259 channels, *Geophys. Res. Lett.*, 34, L18803, doi:10.1029/2007GL030168.
- 1260
- 1261 Schmidt R.H. (1979). A climatic delineation of the “real” Chihuahuan Desert, *J. Arid*
1262 *Environ.*, 2, 243–250.
- 1263 Schütz, L., R. Jaenicke, and H. Pietrek (1981), Saharan dust transport over the North
1264 Atlantic Ocean, in *Desert Dust* edited by T. L. Péwé, pp. 87-100, *Geol. S. Am.*
1265 *S.*, 186, 87-100.
- 1266 Shao, Y., M. R. Raupach, and P. A. Findlater (1993), Effect of saltation bombardment
1267 on the entrainment of dust by wind, *J. Geophys. Res.*, 98(D7), 12719- 12726.
- 1268 Sharma, A. R., S. K. Khard, and K. V. S. Badarinath (2009) Satellite observations of
1269 unusual dust event over North-East India and its relation with meteorological
1270 conditions, *J. Atmos. Solar-Terrestrial Phys.*, 71, 2032-2039.
- 1271 Shinn, E. A., G. W. Smith, J. M. Prospero, P. Betzer, M. L. Hayes, V. Garrison, V.,
1272 and R. T. Barber (2000), African dust and the demise of Caribbean coral
1273 reefs, *Geophys. Res. Lett.*, 27, 3029-3032.
- 1274 Springer, M. E. (1958), Desert pavement and vesicular layer of some soils of the
1275 desert of the Lahontan Basin, Nevada, *Soil Sci. Soc. Am, Proc.*, 22, 63-66.
- 1276 Stout, J. E. (2003), Seasonal variations of saltation activity on a high plains saline
1277 playa: Yellow Lake, Texas, *Phys. Geogr.*, 24, 61-76.
- 1278 Strong, C., J.E. Bullard, C. Dubois, G.H. McTainsh, and M.C. Baddock, (2010),
1279 Impact of wildfire on sand dune ecology and sediments: an example from the
1280 Simpson Desert, Australia, *J. Arid Environ.*, 74, 11, 1577-1581.

- 1281 Sugden, D. E., R. D. McCulloch, A.J.-M Bory, and A.S. Hein (2009). Influence of
1282 Patagonian glaciers on Antarctic dust deposition during the last glacial period,
1283 *Nat. Geo.*, 2, 281-285, doi:10.1038/NGEO474.
- 1284 Sun, D., K. M. Lau, and M. Kafatos (2008). Contrasting the 2007 and 2005 hurricane
1285 seasons: evidence of possible impacts of Saharan dry air and dust on tropical
1286 cyclone activity in the Atlantic basin, *Geophys. Res. Lett.*, 35, L15405.
- 1287 Sweeney, M., V. Etymezian, and E. McDonald (2006). Desert landforms as natural
1288 and anthropogenic dust sources. Paper presented at 6th International
1289 Conference on Aeolian Research, July 2006, University of Guelph, Ontario,
1290 Canada.
- 1291 Tegen, I., and I. Fung (1994), Modeling of mineral dust in the atmosphere – sources,
1292 transport and optical thickness, *J. Geophys. Res.*, 99(D11), 22897-22914.
- 1293 Tegen, I., S. P. Harrison, K. Kohfeld, I. C. Prentice, M. Coe, and M. Heimann (2002),
1294 Impact of vegetation and preferential source areas on global dust aerosol:
1295 results from a model study, *J. Geophys. Res.*, 107, 4576,
1296 doi:10.1029/2001JD000963.
- 1297 Tucker, C. J., D. Grant, and J. Dykstra (2004), NASA's global orthorectified Landsat
1298 data set, *Photogram. Eng. Rem. Sens*, 70, 313-322.
- 1299 Tungsheng, L., D. Menglin, and E. Derbyshire (1996), Gravel deposits on the
1300 margins of the Qinghai-Xizang Plateau, and their environmental significance,
1301 *Palaeogeogr., Palaeoclim., Palaeoecol.*, 120, 59-170.
- 1302 Uno, I. et al. (2006), Dust model intercomparison (DMIP) study over Asia: overview,
1303 *J. Geophys. Res.*, 111, D12213, doi:10.1029/2005JD006575.
- 1304 Urquhart, L.C. (1959), *Civil Engineering Handbook*. McGraw Hill, New York.
- 1305 USDA-NRCS (2006), *U.S. General Soil Map (STATSGO2) for the states of Arizona,*
1306 *New Mexico and Texas*. Available online at <http://soildatamart.nrcs.usda.gov>
1307 Accessed 02/14/2010.
- 1308 USDA-NRCS (2011), *Digital General Soil Map of US: Metadata*. Available online at
1309 <http://soildatamart.nrcs.usda.gov/Metadata.aspx?Survey-US> Accessed
1310 01/04/2011.
- 1311 Viles, H. A., and A. S. Goudie (2007) Rapid salt weathering in the coastal Namib
1312 desert: implications for landscape development, *Geomorphology*, 85, 49-62.

- 1313 Walker, A.L., M. Liu, S.D. Miller, K.A. Richardson, and D.L. Westphal (2009),
1314 Development of a dust source database for mesoscale forecasting in
1315 southwest Asia, *J. Geophys. Res.*, 114, D18207, doi:10.1029/2008JD011541.
- 1316 Wang, X., Z. Dong, J. Zhang, J. Qu, and A. Zhao (2003), Grain size characteristics of
1317 dune sands in the central Taklimakan Sand Sea, *Sed. Geol.*, 161(1-2), 1-14.
- 1318 Wang, X., Z. Zhou, and Z. Dong, (2006), Control of dust emissions by geomorphic
1319 conditions, wind environments and land use in northern China: an
1320 examination based on dust storm frequency from 1960 to 2003,
1321 *Geomorphology*, 81, 292-308.
- 1322 Wang, X., F. Chen, E. Hasi, and J. Li (2008a), Desertification in China: an
1323 assessment, *Earth-Sci. Rev.*, 88, 188-206.
- 1324 Wang, X., D. Zia, T. Wang, X. Xue, and J. Li (2008b), Dust sources in arid and
1325 semiarid China and southern Mongolia: impacts of geomorphological setting
1326 and surface materials, *Geomorphology*, 97(3-4), 583-600.
- 1327 Warren, A. et al. (2007), Dust raising in the dustiest place on Earth, *Geomorphology*,
1328 92, 25-37.
- 1329 Washington, R., M. Todd, N. J. Middleton, and A. S. Goudie, (2003), Dust-storm
1330 source areas determined by the Total Ozone Monitoring Spectrometer and
1331 surface observations, *Ann. Assoc. Am. Geogr.* 93, 297-313.
- 1332 Washington, R. et al. (2006), Links between topography, wind, deflation, lakes and
1333 dust: the case of the Bodélé Depression, Chad, *Geophys. Res. Lett.*, 33,
1334 L09401, doi:10.1029/2006/GL025827.
- 1335 Wentworth, C.K. (1922), A scale of grade and class terms for clastic sediments, *J.*
1336 *Geology*, 30, 377-392.
- 1337 Werner, M., I. Tegen, S.P. Harrison, K.E. Kohfeld, I.C. Prentice, Y. Balkanski, H.
1338 Rodhe, and C. Roelandt (2003). Seasonal and interannual variability of the
1339 mineral dust cycle under present and glacial climate conditions. *J.*
1340 *Geophys. Res.* 107(D24), 4744, doi:10.1029/2002JD002365.
- 1341 Wolff, E.W. et al. (2006), Southern Ocean sea-ice extent, productivity and iron flux
1342 over the past eight glacial cycles, *Nature*, 440(7083), 491-496.
- 1343 Xue, F.M., X.C. Liu, and Y. Ma (2009), Variation characteristics of dust weather in the
1344 hinterland of Taklimakan Desert during 1997-2007, *Desert and Oasis*
1345 *Meteorology*, 3(1), 31-34.

1346 Yang, L. et al. (2008), The Jilantai Salt Lake shorelines in northwestern arid China
1347 revealed by remote sensing images, *J. Arid Environ.*, 72, 861-866.

1348 Yin, D., S. Nickovic, and W. A. Sprigg (2007), The impact of using different land
1349 cover data on wind-blown desert dust modelling results in the southwestern
1350 United States, *Atmos. Environ.*, 41, 2214-2224.

1351 Yoshioka, M. et al. (2007), Impact of desert dust radiative forcing on Sahel
1352 precipitation: relative importance of dust compared to sea surface
1353 temperature variations, vegetation changes and greenhouse gas warming, *J.*
1354 *Climate*, 20(8) 1445-1467, doi:10.1175/JCL14056.

1355 Zakey, A.S., F. Solmon, and F. Giorgi (2006), Development and testing of a desert
1356 dust module in a regional climate model, *Atmos. Chem. Phys. Discussions*, 6,
1357 1749-1792.

1358 Zender, C.S., and E. Y. Kwon (2005), Regional contrasts in dust emission responses
1359 to climate, *J. Geophys. Res.*, 110, D13201, doi:10.1029/2004JD005501.

1360 Zender, C.S., D.J. Newman, and O. Torres, (2003), Spatial heterogeneity in aeolian
1361 erodibility: uniform, topographic, geomorphic and hydrologic hypotheses, *J.*
1362 *Geophys. Res.*, 108(D17), 4543, doi:10.1029/2002JD003,039.

1363 Zobler, L.A. (1986), *A world soil file for global climate modeling*. NASA Technical
1364 Memo 87802.
1365
1366

1367 **Figures**

- 1368 Figure 1: Model of the impact of humid-arid phases on fine sediment (dust)
1369 production/availability and transport and the response of the aeolian
1370 system (simplified and adapted from *Kocurek*, [1998]).
- 1371 Figure 2: Distribution of surface geomorphologies (left hand panel) and their
1372 relative importance for dust emissions (right hand panel) as detailed in
1373 Table 5 for A: the Chihuahuan Desert (modified from *Baddock et al.*,
1374 [2011], B: the Lake Eyre Basin and C: the Taklamakan desert. Right
1375 hand panels for the Chihuahuan Desert and Lake Eyre Basin also
1376 indicate the location of dust plume sources (see text and table 4).
- 1377 Figure 3: The percentage frequency of dust emissions from the different main
1378 surface geomorphologies for the Chihuahuan Desert, the Lake Eyre
1379 Basin and the western Sahara for time periods given in table 4.
- 1380 Figure 4: Annual variability of the frequency (%) of dust emissions from different
1381 surface geomorphologies for A: the Chihuahuan Desert 2001-2009,
1382 and B: the Lake Eyre Basin 2003-2006.
- 1383 Figure 5: Maps of the Chihuahuan Desert (left hand panels) and Lake Eyre
1384 Basin (right hand panels) showing the percentage of each 0.5 x 0.5°
1385 grid cell containing A: ephemeral and dry lakes [1b-d], B: low relief,
1386 unarmoured, unincised alluvial deposits [3d], and C, D, E: surface
1387 geomorphologies with low, medium and high potential emissions
1388 respectively (where aeolian sand dunes [5b] are classed as medium;
1389 see text).
- 1390 Figure 6: The distribution of aeolian sand dunes [5b] in the Lake Eyre Basin
1391 shown as a percentage of different-sized grid cells. A: 0.25 x 0.25°, B:
1392 0.5 x 0.5°, C: 1 x 1°, D: 2 x 2°.
- 1393
- 1394

1395 **Tables**

1396 Table 1: Qualitative indicators of sediment texture and associated erodibility
1397 and dust generation potential.

1398 Table 2: Identification of surface geomorphologies and their contribution to dust
1399 emissions in space and time.

1400 Table 3: Comparison of geomorphic classifications used for attributing dust
1401 emissions. % DPF = % dust plume frequency, Mean DSF = dust storm
1402 frequency = mean number dust storms days per year. *local name.

1403 Table 4: Summary of dust point source data for three regions.

1404 Table 5: Surface area covered by different geomorphologically-defined
1405 emission sources and the frequency (%) with which dust plumes are
1406 observed from those surfaces. Dust plume data for time periods given
1407 in Table 4. Not all data are available for each region, see text for
1408 details. Limits to area of Chihuahuan Desert from *Schmidt* [1979],
1409 Lake Eyre Basin watershed determined using GeoScience Australia
1410 catchment boundary, Taklamakan Desert defined as land <1400 m
1411 altitude within the Tarim Basin.

1412

1413

1414

1415

1416

1417

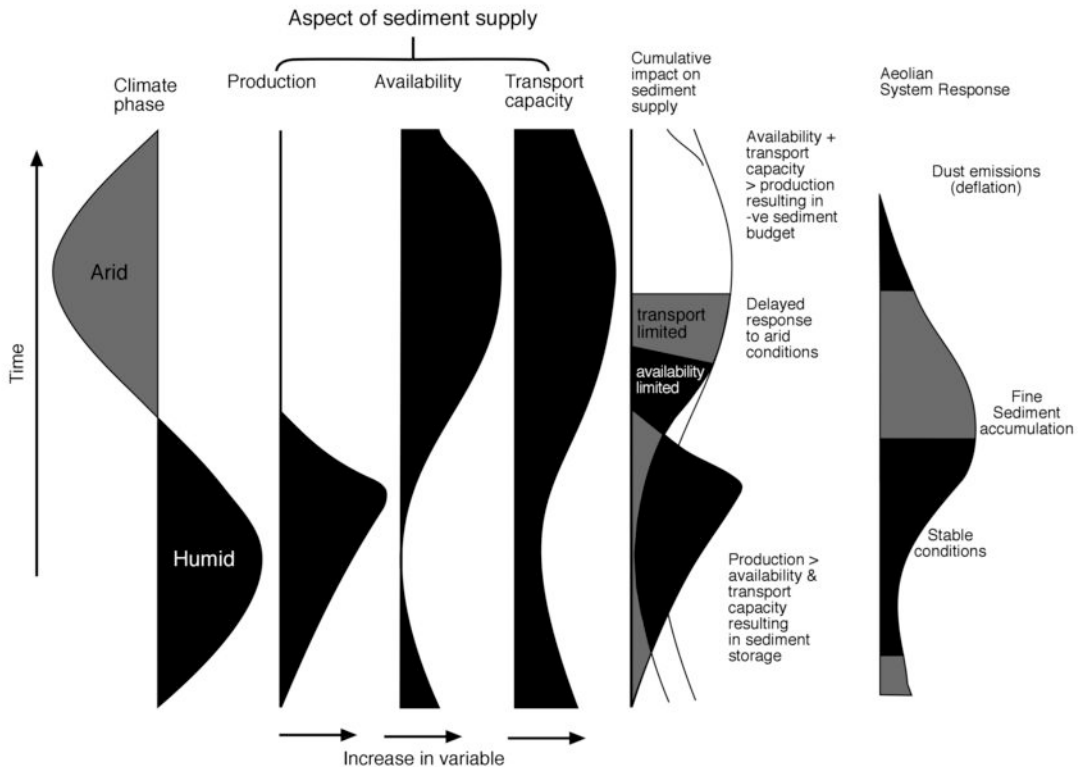
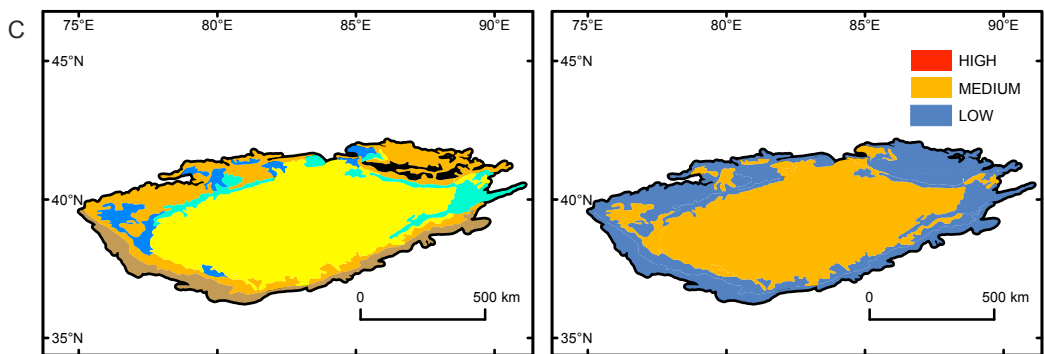
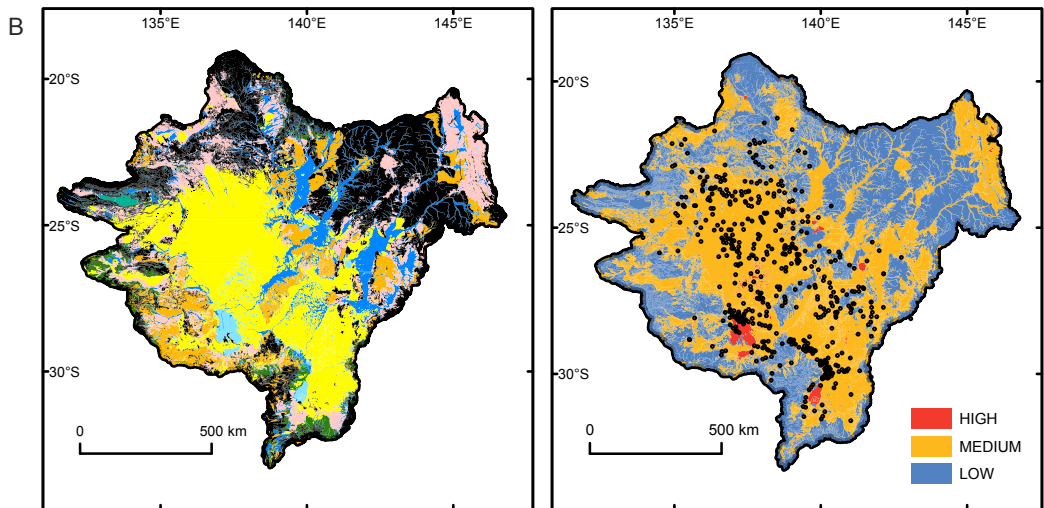
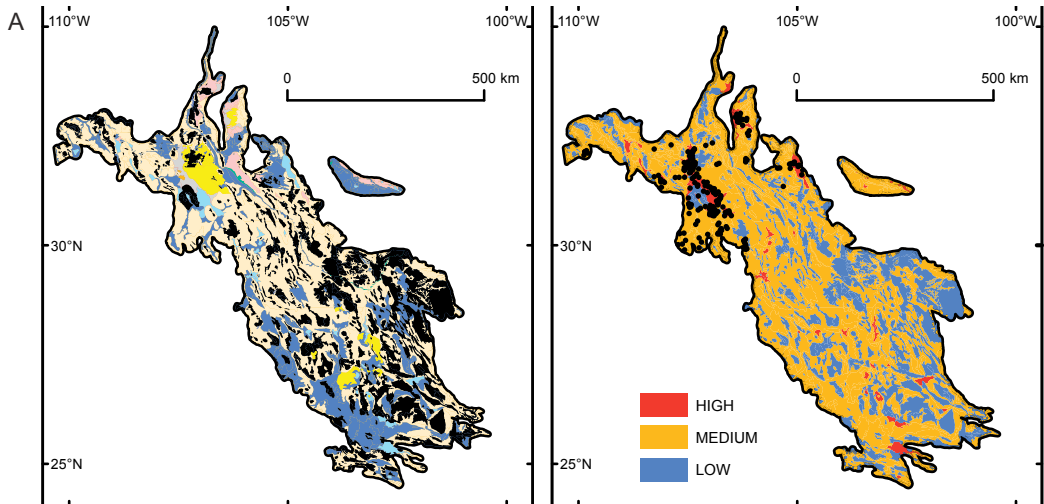


Figure 1: Model of the impact of humid-arid phases on fine sediment (dust) production/availability and transport and the response of the aeolian system (simplified and adapted from Kocurek, [1998]).



Geomorphological Map Legend













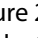
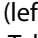
- | | |
|---|--|
|  1a - Wet lake |  3c - Low relief alluvial (unarmoured, incised) |
|  1b - Ephemeral lake |  3d - Low relief alluvial (unarmoured, unincised) |
|  1c - Dry lake, consolidated |  4 - Stony surface |
|  1d - Dry lake, unconsolidated |  5a - Sand sheet |
|  2b - High relief alluvial (armoured, unincised) |  5b - Aeolian sand dunes |
|  2c - High relief alluvial (unarmoured, incised) |  6 - Loess |
|  2d - High relief alluvial (unarmoured, unincised) |  7 - Low emission surfaces |

Figure 2: Distribution of surface geomorphologies (left hand panel) and their relative importance for dust emissions (right hand panel) as detailed in Table 5 for A: the Chihuahuan Desert (modified from *Baddock et al.*, [2011], B: the Lake Eyre Basin and C: the Taklamakan Desert. Right hand panels for the Chihuahuan Desert and Lake Eyre Basin also indicate the location of dust plume sources (see text and Table 4).

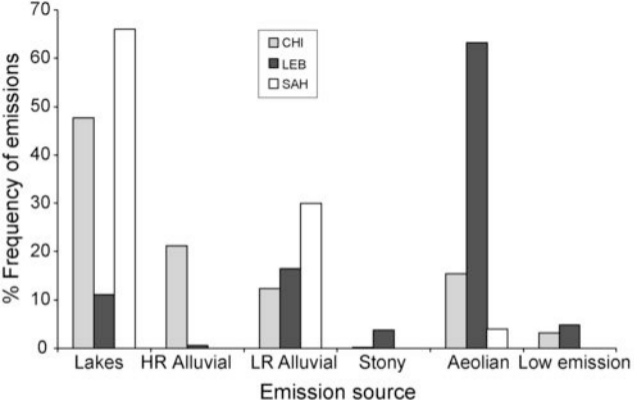


Figure 3: The percentage frequency of dust emissions from the different main surface geomorphologies for the Chihuahuan Desert, the Lake Eyre Basin and the western Sahara for time periods given in table 4.

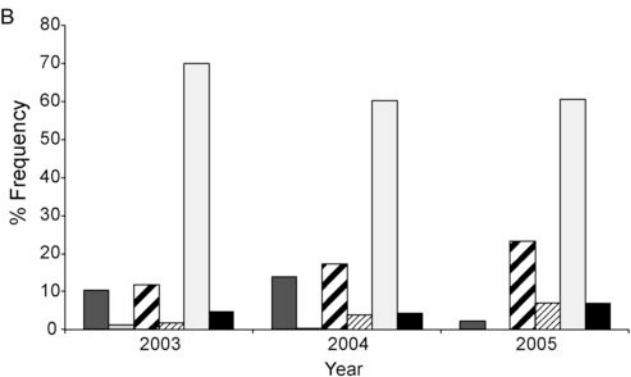
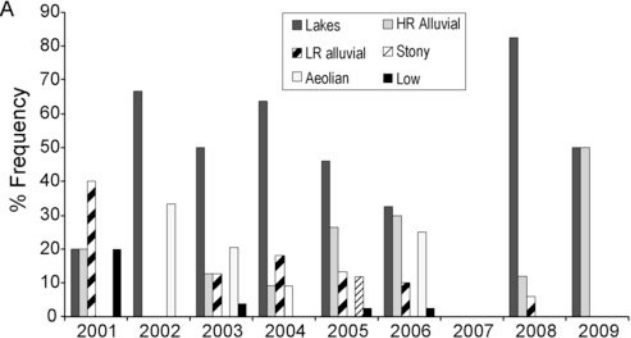
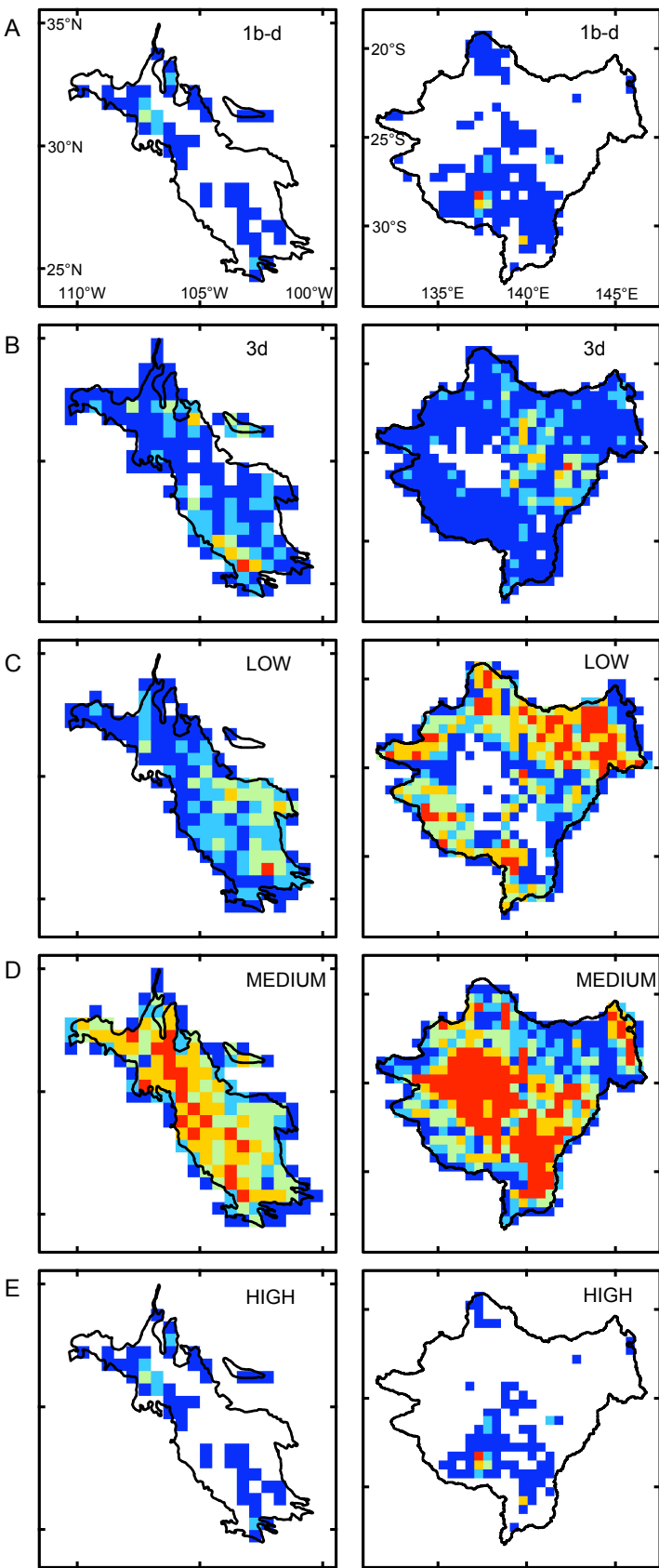


Figure 4: Annual variability of the frequency (%) of dust emissions from different surface geomorphologies for A: the Chihuahuan Desert 2001-2009, and B: the Lake Eyre Basin 2003-2006



% 1 - 20 20 - 40 40 - 60 60 - 80 80 - 100

Figure 5: Maps of the Chihuahuan Desert (left hand panels) and Lake Eyre Basin (right hand panels) showing the percentage of each $0.5 \times 0.5^\circ$ grid cell containing A: ephemeral and dry lakes [1b-d], B: low relief, unarmoured, uncised alluvial deposits [3d], and C, D, E: surface geomorphologies with low, medium and high potential emissions respectively (where aeolian sand dunes [5b] are classed as medium; see text).

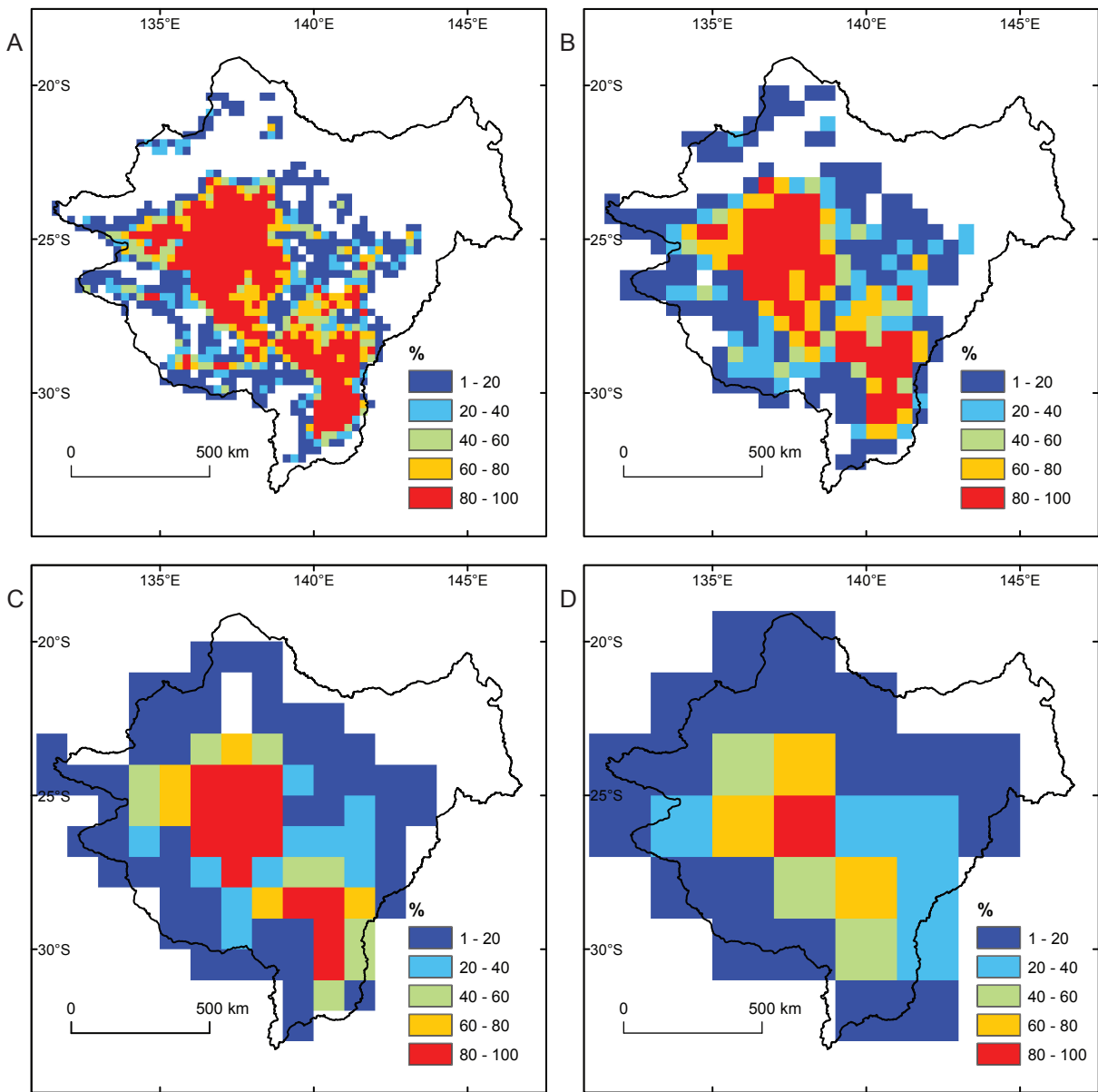


Figure 6: The distribution of aeolian sand dunes [5b] in the Lake Eyre Basin shown as a percentage of different sized grid cells. A: 0.25 x 0.25° B: 0.5 x 0.5° C: 1 x 1° D: 2 x 2°.

Table 1: Qualitative indicators of sediment texture and associated erodibility and dust generation potential.

Sediment texture	Wind Erodibility	Dust generation potential	Example sedimentary environments
Mixed sand/gravel	Low	Low	Proximal alluvial fans; non-emitting surfaces
Mixed clay/silt + gravel	Low	Moderate	Stony surfaces, distal alluvial fans
Sand	High	Moderate-variable	Sandy aeolian deposits, sand sheets, sand dunes
Mixed sand/silt	High	High	Source-proximal loess, fluvially-coupled ephemeral lakes
Silt/clay	High	Low	Ephemeral + dry unconsolidated lakes, source-distal loess
Sand/clay	High	High	Fluvially-coupled ephemeral lakes, margins of ephemeral and dry lakes, some dry or ephemeral lake/playa surfaces

Table 2: Identification of surface geomorphologies and their contribution to dust emissions in space and time.

	Emission sources	Typical soil textures	Limitation on emissions	Dominant temporal pattern	Importance for dust emissions [<i>value used for Figs 2 and 6 where a range is indicated</i>]
Lakes	1a Wet	Sand, Silt, Clay	Availability-limited	No variability	Low
	1b Ephemeral	Silt, Clay	Supply-limited	Periodic emissions triggered sediment supply and reworking following high rainfall	High (if sandblasting) – Medium [<i>high</i>]
	1c Dry – consolidated	Silt, Clay	Availability-limited	No systematic variability	Low
	1d Dry – non consolidated	Silt, Clay	Transport capacity limited	Emission when wind velocity > entrainment threshold	High (if sandblasting) – medium [<i>high</i>]
High Relief Alluvial Systems	2a Armoured, incised	Mega-gravel, Gravel, Sand	Availability-limited	No systematic variability	Low
	2b Armoured, unincised	Mega-gravel, Gravel, Sand	Availability-limited	No systematic variability	Low
	2c Unarmoured, incised	Gravel, Sand, Silt, Clay	Supply-limited	Periodic emissions triggered by sediment supply and reworking following high rainfall	Medium
	2d Unarmoured, unincised	Sand, silt, clay	Supply-limited	Periodic emissions triggered by sediment supply and reworking following high rainfall	Medium-High [<i>medium</i>]

Table 2 (continued)

Low Relief Alluvial Systems	3a Armoured – incised	Gravel, Sand,	Availability-limited	No systematic variability	Low
	3b Armoured - unincised	Gravel, Sand, Silt, Clay	Supply-limited	Periodic emissions triggered by sediment supply and reworking following high rainfall	Medium
	3c Unarmoured – incised	Sand, Silt, Clay	Transport capacity limited	Emission when wind velocity > entrainment threshold	Low
	3d Unarmoured– unincised	Sand, Silt, Clay	Supply-limited	Periodic emissions triggered by sediment supply and reworking following high rainfall	Medium
	4 Stony surfaces: low angle surfaces; not connected to fluvial source of fines	Gravel, Sand, Silt, Clay	Availability limited	No systematic variability	Low
Aeolian Systems	5a Sand Sheet	Sand	Supply- and/or availability-limited	Variability dependent on vegetation cover, water table etc.	Low to medium [<i>medium</i>]
	5b Aeolian sand dunes	Sand	Supply- and/or availability-limited	Variability dependent on dune type, dynamics, sedimentology and palaeohistory	Low to high [<i>medium</i>]
	6 Loess	Silt, Clay	Availability-limited	Variability dependent on vegetation cover	Low to medium [<i>low</i>]

7 Low emission surfaces - bedrock, rocky slopes, duricrust (snow/ice permanent cover)	Mega-gravel, Gravel, Sand, Silt, Clay	Supply-limited	No systematic variability	Low
---	---------------------------------------	----------------	---------------------------	-----

Table 3: Comparison of geomorphic classifications used for attributing dust emissions. % DPF = % dust plume frequency, Mean DSF = mean number of dust storms days per year. *local name.

SW North America <i>Lee et al., [2009]</i>		Lake Eyre Basin <i>Bullard et al., [2008]</i>		Western Sahara <i>Drake et al., [2008]</i>		Northern China <i>Wang et al., [2006]</i>	
Surface	% DPF	Surface	% DPF	Surface	% DPF	Surface	Mean DSF
Playa	21	Dry lakes	29	Palaeolakes	54		
				Palaeorivers	17		
		Rivers & floodplains	26	Floodplains & inland deltas	2		
		Stony desert (gibber*)	2	Stony desert (hamada*)	1	Stony desert (gobi*)	9
		Sand dunes	39	Sand dunes	1	Sand dunes (mobile)	6
						Sand dunes (semi-mobile)	14
Agricultural lands	40			Agricultural lands	5	Agricultural lands	3
Rangelands	34					Grasslands	4
Other	5	Other	5	Other	1	Oasis	11

Table 4: Summary of dust point source data for three regions.

	Chihuahuan Desert	Lake Eyre Basin	Western Sahara Desert
Data type	MODIS Terra or Aqua	MODIS Terra or Aqua	MODIS Terra
Spatial resolution used (km)	0.25 x 0.25	1 x 1	1 x 1
Additional processing	None	Bispectral split window analysis (Ackerman, 1997)	Miller (2003) Dust Index
Dust event selection criteria	Reduction in visibility at meteorological station (combined with low humidity and high wind)	Visibility \leq 1 km at meteorological station	Dust storm visible in MODIS colour composite.
Period examined	January 2001-December 2009	July 2003-June 2006	April-July 2003
Number dust event days	26	27	11
Number traceable individual dust plumes	217	529	98

Table 5: Surface area covered by different geomorphologically-defined emission sources and the frequency (%) with which dust plumes are observed from those surfaces. Dust plume data for time periods given in Table 4. Not all data are available for each region, see text for details. Limits to area of Chihuahuan Desert from *Schmidt* [1979], Lake Eyre Basin watershed determined using GeoScience Australia catchment boundary, Taklamakan Desert defined as land <1400 m altitude within the Tarim Basin.

Emission sources		Chihuahuan Desert				Lake Eyre Basin				Sahara		Taklamakan
		Area km ²	Dust plumes			Area km ²	Dust plumes			Dust plumes		Area km ²
			Freq	%	Plumes per 1km ⁻²		Freq	%	Plumes per 1km ⁻²	Freq	%	
Lakes	1a Wet	243	0	0	0							
	1b Ephemeral	8905	64	29.5	0.0072	43818	58	11	0.0013	3	3	
	1c Dry – consolidated											7.1
	1d Dry – non consolidated	3564	40	18.4	0.0112					62	63	
High relief alluvial systems	2a Armoured, incised											
	2b Armoured, unincised					35251	3	0.6	0.0001			
	2c Unarmoured, incised	32	0	0	0							
	2d Unarmoured, unincised	138728	45	20.7	0.0003							
Low relief alluvial systems	3a Armoured – incised											
	3b Armoured - unincised											
	3c Unarmoured – incised	436	0	0	0	7571	-	-	-	5	5	
	3d Unarmoured– unincised	64683	26	12.0	0.0004	172401	87	16.5	0.0005	24	25	5.5

Table 5 (continued)

	4	Stony surfaces	141	1	0.5	0.0071	132531	20	3.8	0.0002			22.2
Aeolian systems	5a	Sand Sheet	7178	4	1.8	0.0006	161747	30	5.7	0.0002	2	2	
	5b	Aeolian sand dunes	9450	30	13.8	0.0032	305888	304	57.6	0.0010	2	2	54.5
	6	Loess											8.8
	7	Low emission surfaces	89090	7	3.2	0.0001	330404	26	4.9	0.0001			1.9